



This is a repository copy of *Flexible operation of post-combustion CO<sub>2</sub> capture at pilot scale with demonstration of capture-efficiency control using online solvent measurements* .

White Rose Research Online URL for this paper:  
<http://eprints.whiterose.ac.uk/128252/>

Version: Accepted Version

---

**Article:**

Tait, P., Buschle, B., Milkowski, K. et al. (3 more authors) (2018) Flexible operation of post-combustion CO<sub>2</sub> capture at pilot scale with demonstration of capture-efficiency control using online solvent measurements. *International Journal of Greenhouse Gas Control*, 71. pp. 253-277. ISSN 1750-5836

<https://doi.org/10.1016/j.ijggc.2018.02.023>

---

**Reuse**

This article is distributed under the terms of the Creative Commons Attribution-NonCommercial-NoDerivs (CC BY-NC-ND) licence. This licence only allows you to download this work and share it with others as long as you credit the authors, but you can't change the article in any way or use it commercially. More information and the full terms of the licence here: <https://creativecommons.org/licenses/>

**Takedown**

If you consider content in White Rose Research Online to be in breach of UK law, please notify us by emailing [eprints@whiterose.ac.uk](mailto:eprints@whiterose.ac.uk) including the URL of the record and the reason for the withdrawal request.



[eprints@whiterose.ac.uk](mailto:eprints@whiterose.ac.uk)  
<https://eprints.whiterose.ac.uk/>

1 **Flexible operation of post-combustion CO<sub>2</sub> capture at pilot scale with demonstration of capture-**  
2 **efficiency control using online solvent measurements.**

3  
4 **Name(s) of author(s): Paul Tait<sup>[a]\*</sup>, Dr Bill Buschle<sup>[a]</sup>, Dr Kris Milkowski<sup>[b]</sup>, Dr Muhammad Akram<sup>[b]</sup>,**  
5 **Prof Mohamed Pourkashanian<sup>[b]</sup>, Dr Mathieu Lucquiaud<sup>[a]</sup>**

6 **Affiliation: The University of Edinburgh<sup>[a]</sup>, The University of Sheffield<sup>[b]</sup>**

7  
8 **Keywords:** Post-combustion, pilot, flexibility, control, coal

9  
10 **Abstract**

11 Flexible post-combustion carbon capture and storage (CCS) has the potential to play a significant part in  
12 the affordable decarbonisation of electricity generation portfolios. PCC plant operators can modify capture  
13 plant process variables to adjust the CO<sub>2</sub> capture level to a value which is optimal for current fuel cost,  
14 electricity selling price and CO<sub>2</sub> emissions costs, increasing short-term profitability. Additionally, variation  
15 of the level of steam extraction from the generation plant can allow the capture facility to provide additional  
16 operating flexibility for coal-fired power stations which are comparatively slow to change output.

17 A pilot-scale test campaign investigates the response of plant operating parameters to dynamic scenarios  
18 which are designed to be representative of pulverized coal plant operation. Online sensors continuously  
19 monitor changes in rich and lean solvent CO<sub>2</sub> loading (30%wt monoethanolamine). Solvent loading is likely  
20 to be a critical control variable for the optimisation of flexible PCC operation, and since economic and  
21 operational boundaries can change on timescales 30mins or shorter, the development of methods for rapid,  
22 continuous online solvent analysis is key. Seven dynamic datasets are produced and insights about plant  
23 response times and hydrodynamics are provided. These include power output maximization, frequency  
24 response, power output ramping and a comparison between two plant start-up strategies.

25 In the final dynamic operating scenario, control of CO<sub>2</sub> capture efficiency for a simple reboiler steam  
26 decoupling and reintroduction event is demonstrated using only knowledge of plant hydrodynamics and  
27 continuous measurement of solvent lean loading. Hot water flow to the reboiler is reduced to drop the  
28 capture efficiency. The “target” value for the minimum capture efficiency in the scenario was set at 30%,  
29 but a minimum CO<sub>2</sub> capture efficiency of 26.4% was achieved. While there remains scope for improvement  
30 this represents a significant practical step towards the control of capture plant using online solvent  
31 concentration and CO<sub>2</sub> measurements, and the next steps for its further development are discussed.

32  
33  
34 **1. Introduction**

35 Despite the continuing phase-out of coal power generation in Europe it is likely to remain an important  
36 source of electricity in Asia, Africa and the Americas through 2040 and beyond (IEA, 2015) Carbon capture  
37 and storage (CCS) has the potential to significantly limit the emissions from coal and gas-fired power  
38 stations, reducing the cost and mitigating the worst effects of dangerous climate change (IPCC, 2014). Post-  
39 combustion capture (PCC) applied to coal-fired power stations is a proven technology for the reduction of  
40 CO<sub>2</sub> from flue gas, but there are outstanding questions regarding how the process responds to changes in  
41 generation plant output.

42 Coal-fired plants are less likely to provide dispatchable services for rapid response to spikes in electricity  
43 demand due to their slower ramp rate than modern NGCCs. However, the plants are capable to do so if  
44 needs be, and are increasingly likely to participate in load-following operations or operate in a two-shifting  
45 regime. In this regime the plant is shut down at night due to reduced demand and restarted in the morning  
46 when the demand is higher. Flexibility in capture plant operation is critical if it is to respond to these  
47 dynamic generation events effectively.

48 Capture plant flexibility also allows coal-fired power stations to maximise the electricity available for  
49 transmission while the plant is operating at baseload. Errey et al (2014) demonstrates the value of CO<sub>2</sub>  
50 capture plants varying their capture efficiency in response to changes in electricity selling price. Mac  
51 Dowell (2015) and Flø (2016) use dynamic models to investigate various capture plant operation strategies  
52 to capitalise on volatile electricity selling price while maintaining an average CO<sub>2</sub> capture efficiency which  
53 is close to 90% over 24 hours. The model used by Flø (2016) is validated against flexibility tests done at  
54 the Brindisi pilot published previously by Mangiaracina et al. (2014). However, the availability of dynamic  
55 plant performance data in open literature is very limited and the lack of public-domain dynamic plant data

56 makes the validation of these strategies problematic (Bui, 2014), especially for dynamic scenarios which  
57 are more complex than a step-change in a single plant parameter.  
58 Furthermore, the implementation of these operational strategies requires a robust process control system  
59 to achieve optimised performance when manipulating reboiler steam input to capitalise on fluctuating  
60 electricity selling price, or responding to a dynamic generation plant event (Mac Dowell, 2015; Flø 2016).  
61 Tait et al (2016) suggest that active control of the real-time solvent capacity via manipulation of solvent  
62 flow rate and/or reboiler heat input, combined with continuous measurement of lean and rich solvent CO<sub>2</sub>  
63 loading could be used to control CO<sub>2</sub> capture efficiency during dynamic operations.  
64 This work details the implementation of dynamic scenarios at pilot plant scale. The test campaign shares  
65 some similarity with previously published work on post-combustion capture on NGCC plant by Tait et al  
66 (2016) but with several key differences. This work focuses on coal generation; the dynamic scenarios are  
67 based on operating data from real coal plant and on operating modes which are most relevant to post-  
68 combustion capture on coal. The test facility is purpose-built for CO<sub>2</sub> capture and the reboiler design is  
69 significantly different to that described in Tait et al (2016), allowing comparisons to be made between how  
70 different pilot-plant design and configuration affects the response to dynamic operations. The deployment  
71 of two online solvent sensors allows for continuous measurement of both rich and lean loading to be made.  
72 Seven dynamic operating scenarios are implemented. This includes two different shutdown-startup  
73 couplings, frequency response, load-following and two capture bypass events. These scenarios are used to  
74 provide insights about plant hydrodynamics and response to dynamic scenarios while passively  
75 monitoring changes in solvent loading with the online solvent sensors. The knowledge of plant dynamics  
76 gained over the course of the test campaign is used in a final scenario in which online lean solvent loading  
77 measurements are used to demonstrate control of CO<sub>2</sub> capture efficiency following a steam decoupling  
78 event.

79

## 80 **2. Overview of Test Facility**

81 The amine technology CO<sub>2</sub> capture plant which was previously installed at Didcot power station by RWE is  
82 now located at the PACT facilities of the UKCCSRC at the University of Sheffield. The plant is purpose-built  
83 for CO<sub>2</sub> capture operations and has been upgraded several times since 2012. A simplified layout of the  
84 capture plant is shown in Fig. 1. The absorber contains 6.50m of 300mm diameter Sulzer Mellapak CC3  
85 packing, while the desorber contains 6m of Intalox IMTP 25 random packing and is 300mm in diameter.  
86 There are several options for flue gas injection – the facility can be connected to a biomass burner, a gas  
87 turbine or a gas mixing skid which can create synthetic flue gas from air/N<sub>2</sub> and CO<sub>2</sub>. For the duration of  
88 the test campaign, a mixture of ambient air with approx. 12% CO<sub>2</sub> from the gas mixing skid is used to  
89 simulate flue gas from a coal-fired power station. Gas ordinarily flows through an FGD wash column prior  
90 to entering the absorber (Akram, 2016), but due to consistent problems with water condensation and  
91 buildup in the pipework between the FGD and absorber inlet, the FGD is bypassed for the duration of the  
92 test campaign. For all tests, the flue gas entering the absorber is unsaturated and has water content approx.  
93 1% of total volume. This causes the plant to lose water through the absorber gas outlet, resulting in an  
94 increase in nominal amine concentration of 2-3% w/w per day. The effect of this on plant reboiler duty is  
95 discussed in section 3.2.

96 To make up for these water losses the plant is topped up with water manually if necessary at the beginning  
97 of the operating day.

98

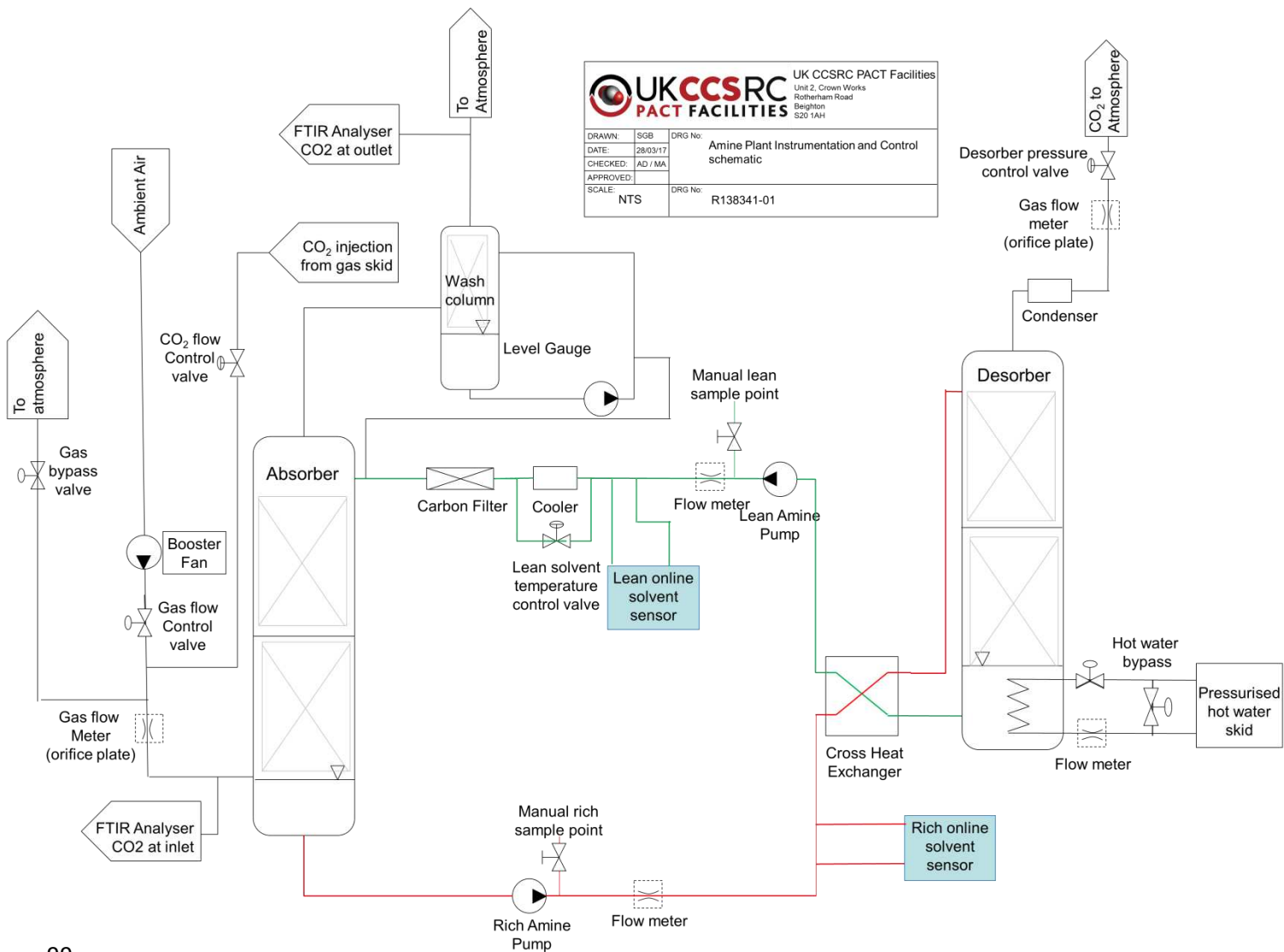


Fig. 1. Process flow diagram of amine plant (Akram, 2017)

99  
 100  
 101  
 102  
 103  
 104  
 105  
 106  
 107  
 108  
 109  
 110  
 111

The plant uses pressurised hot water to regenerate rich solvent. The reboiler, shown in Fig. 2, consists of a large overspill tank containing a heating element, through which pressurised water at approx. 124°C is pumped. At the end of the reboiler tank furthest from the desorber, solvent spills over a baffle to feed the lean solvent pump. The pump is protected by a sensor which will trip if the liquid level in this section falls below a given threshold, shutting down the plant. The total solvent inventory of the plant is approx. 600l, the majority of which resides in the reboiler during operation. The absorbing solvent used for the duration of the test campaign is 30% Monoethanolamine (MEA), though the nominal amine concentration varies between 28% and 35% due to the aforementioned water losses.

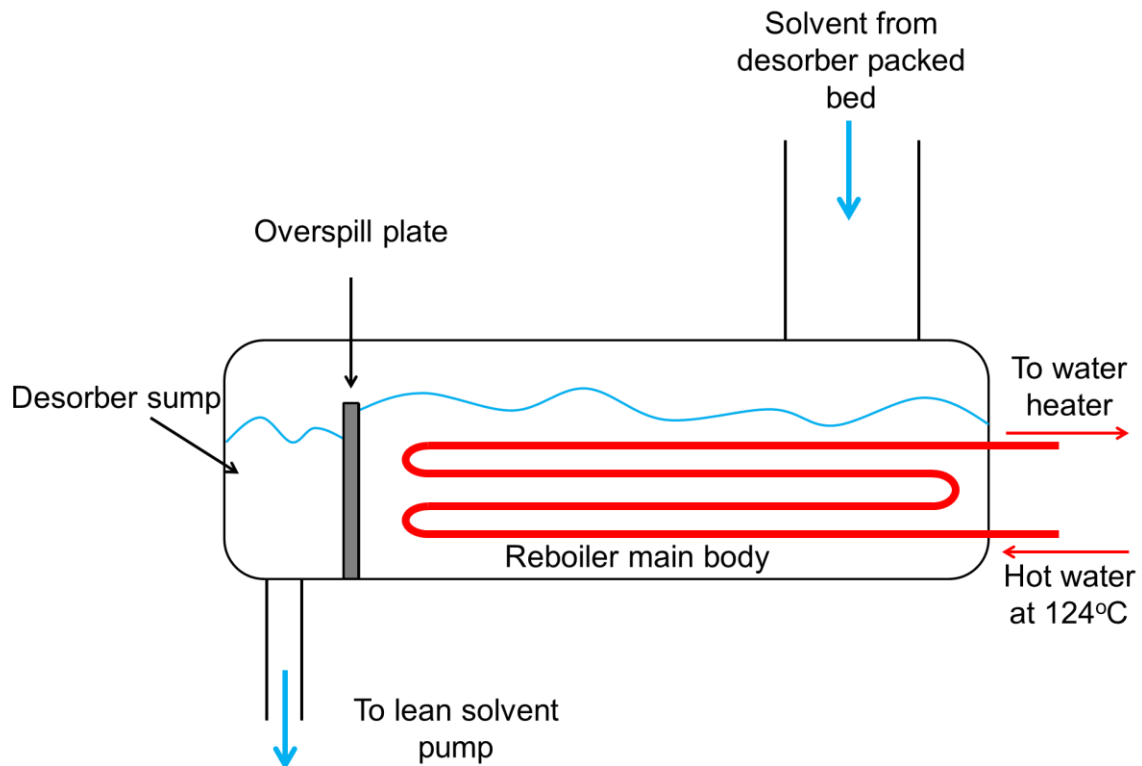


Fig. 2. Reboiler design at UKCCSRC PACT

112  
113  
114

115 The gas flow is comprised of ambient air which is enriched with CO<sub>2</sub> to the required concentration via  
116 injection and checked via a Fourier Transform infra-red (FT-IR) spectroscopy analyser at the absorber gas  
117 inlet. A second FT-IR device analyses the gas composition at the absorber outlet. As the only two available  
118 FT-IR systems are required at the absorber inlet and outlet for the determination of CO<sub>2</sub> capture efficiency,  
119 it is not possible to determine the CO<sub>2</sub> mass flow at the desorber outlet.

120 Solvent flow rate is controlled via individually-controlled valves located after the rich and lean solvent  
121 pump. The valves can be controlled via a flow rate setpoint or opened and closed manually. During solvent  
122 flow rate changes there is a considerable risk of plant shutdown as the solvent level in the absorber sump  
123 may fall below the trip switch threshold, making fine control and ramping very difficult to implement. For  
124 this reason only large step-changes in solvent flow are used in the test campaign.

125 A bypass valve allows the flow of pressurised hot water to the reboiler to be adjusted using a PID controller.  
126 The hot water pump has an operating range of 0-10m<sup>3</sup>/hr and while the flowmeter is unable to detect any  
127 flow below approx. 3.0m<sup>3</sup>/hr, below this value the PID controller can be switched off allowing the valve  
128 position to be adjusted manually. However, as there is no flow measurement determining the hot water  
129 flow rate between 0-3m<sup>3</sup>/hr is a matter of guesswork.

130 Desorber pressure setpoint is adjusted via a PID controller by opening or closing the valve at the top of the  
131 desorber. For all scenarios in this work, the desorber pressure setpoint was 0.4 bar<sub>g</sub>. Desorber pressure  
132 fluctuates between around 0.37-0.47 bar<sub>g</sub> at baseload flow conditions.

133

134 At baseload conditions the cross-flow heat exchanger provides a temperature increase of approx. +47°C to  
135 the rich solvent entering the desorber and a decrease of approx. -47°C to the lean solvent entering the  
136 absorber. This is sufficient to bring the lean solvent down from 99°C at the desorber sump outlet to around  
137 52°C, so further cooling is required to reduce the temperature to 40°C at the absorber inlet. Solvent enters  
138 the desorber at approx. 98°C at baseload conditions. Absorber inlet temperature is maintained at 40°C  
139 using a PID-controlled cooler and bypass valve which is connected to the PLC system. There is very little  
140 variation in lean solvent temperature at the absorber inlet once the temperature of lean solvent coming  
141 from the cross-heat exchanger is greater than 40°C.

142  
 143  
 144  
 145  
 146  
 147  
 148  
 149  
 150  
 151  
 152  
 153  
 154  
 155  
 156  
 157  
 158  
 159  
 160

**3. Methodology and Preparation**  
**3.1 Solvent Mixing Experiments**

Solvent circulation times and mixing effects have been shown to affect plant response to dynamic operations (Tait et al, 2016), so prior knowledge of plant hydrodynamics is required to fully account for changes in capture efficiency, absorber temperature profile, lean loading and rich loading over the course of each dynamic scenario.

Four conductivity probes, two on each of the rich and lean solvent lines, were installed. The pair of probes installed on the rich line monitored the outlet of the absorber and inlet of the desorber, while the pair of probes installed on the lean solvent line monitored the outlet of the desorber and the inlet of the absorber. Ideally the conductivity probes would be installed as close as possible to the inlets and outlets of the absorber and desorber. However, due to difficulties in installing the conductivity probes at heights all of the probes were installed at ground level. This meant that the distance between the pair of probes was shorter as compared to if they were installed at the inlets to absorber and desorber columns. For this reason it is not possible to determine the circulation between the lean solvent pump > absorber inlet or rich solvent pump > desorber inlet, but valuable information about solvent mixing and total circulation time can still be obtained.

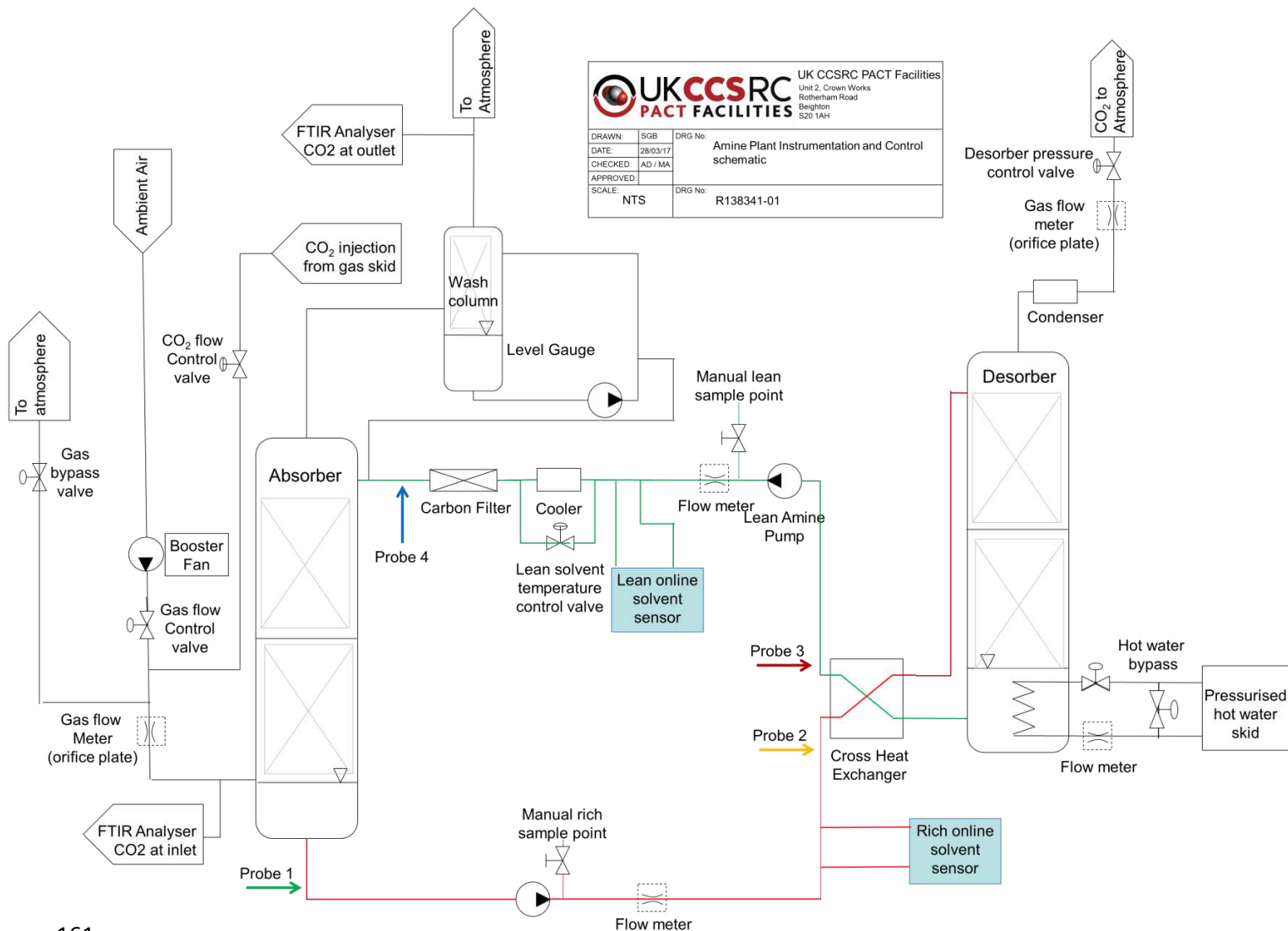


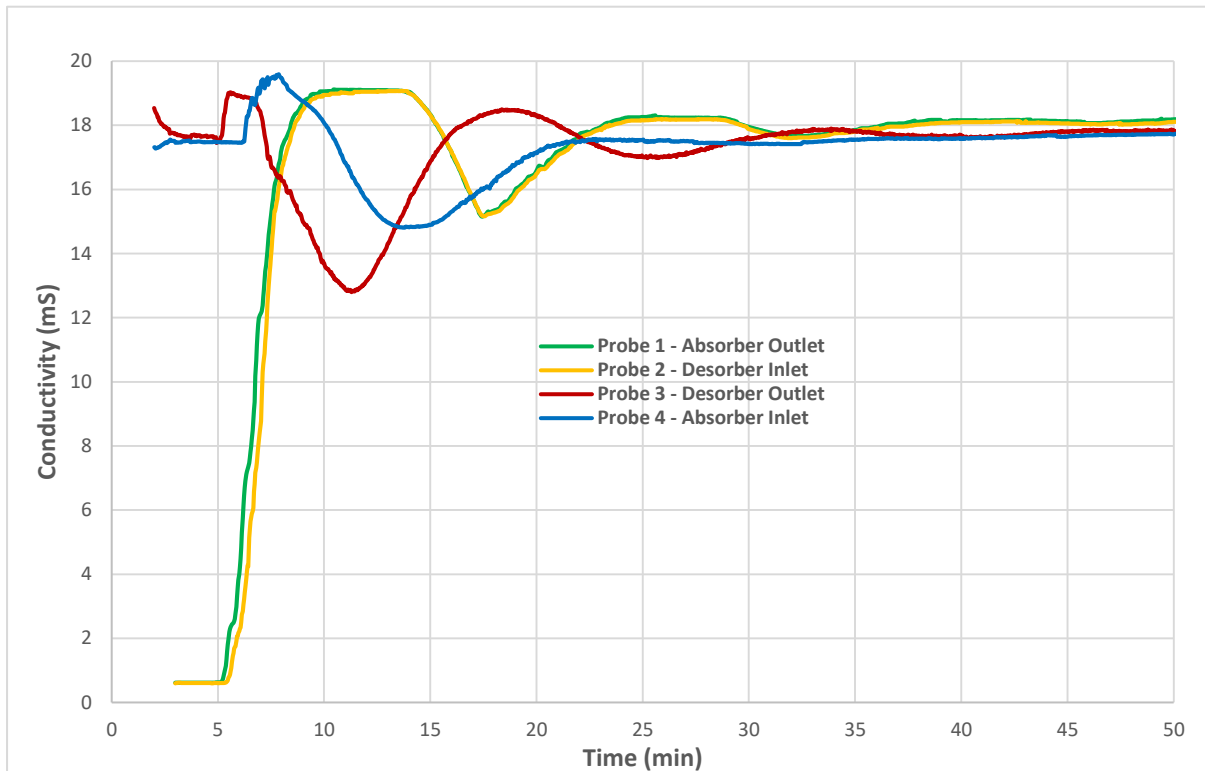
**Fig. 3 Plant PFD with conductivity probe locations**

161  
 162  
 163

164 A batch of amine solvent (between 30-40%wt MEA, approx. 400l) is isolated in the desorber sump.  
165 Deionised water (approx. 70l) is added to the absorber sump. The solvent pumps are started at t=0. As pure  
166 water mixes with amine solvent, the conductivity decreases. By observing the conductivity at each of these  
167 points it is possible to estimate the circulation time between them and the duration required for the solvent  
168 inventory to become fully mixed.

169 Tests were carried out at the initially proposed baseload flowrate (1200l of solvent/hr), but a flow rate of  
170 only 1000l/hr was necessary to achieve >90% capture (see section 3.2).

171  
172  
173  
174



175  
176 **Fig. 4. Liquid circulation experiments**  
177

178 Due to their close proximity in the liquid line (see fig. 3), pair of probes installed on the rich solvent line  
179 (probe 1-absorber outlet/probe 2- desorber inlet ), conductivity values measured by the pair follow each  
180 other closely (see fig. 4). However, there is a noticeable difference in the conductivity values measured by  
181 the pair of probes installed on the lean solvent line (probe 3- desorber outlet/probe 4-absorber inlet) which  
182 may indicate a small amount of solvent mixing taking place within the line, or may be due to the lean solvent  
183 pump starting up and stabilising more slowly than the rich.

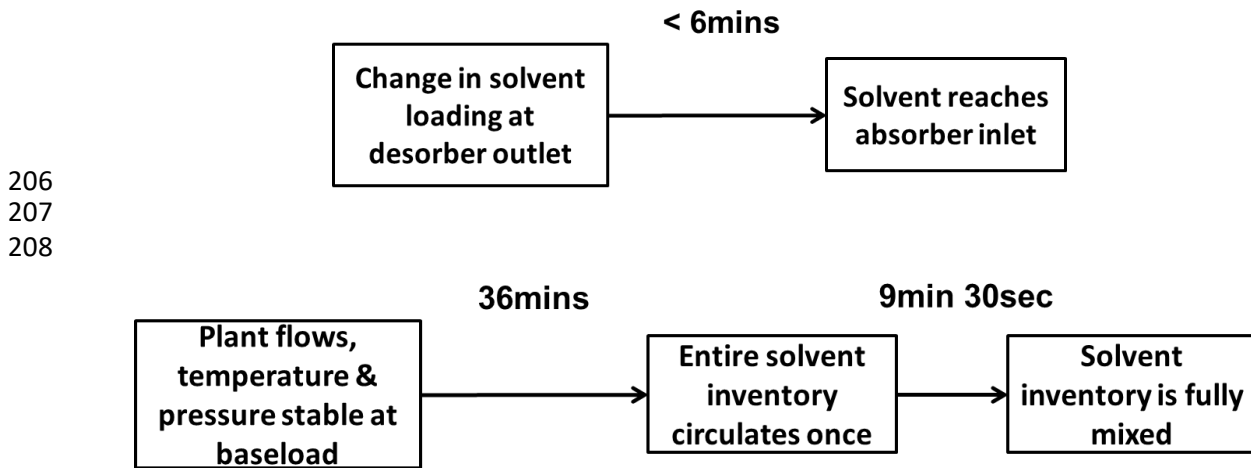
184 Conductivity at the absorber outlet (probe 1) begins to increase at t=5min. This indicates that the minimum  
185 time required for a small batch of solvent located at the desorber outlet (probe 3) to circulate to the  
186 absorber sump and begin mixing with the sump's existing solvent inventory is 5min. Conductivity at the  
187 desorber outlet (probe 3) begins to decrease at t=5min 30sec, indicating that the time required for a batch  
188 of solvent to circulate from the absorber outlet (probe 1) to the reboiler and begin mixing with the solvent  
189 inventory is 5min 30sec. The entire solvent inventory requires 37-38min to become fully mixed, which is  
190 7min more than the estimated time of 30 min required for a batch of solvent to fully circulate the plant at  
191 this flow condition, based on vessel volumes and total solvent inventory. The implications for dynamic  
192 operations are:

- 193 1. During operation, the solvent spends approx. 2/3 of the time residing in the reboiler or absorber  
194 sump. This allows ample time for the solvent to become well mixed. Therefore it is not anticipated

195 that after, for example, reintroduction of hot water to the reboiler after a decoupling event, large  
 196 additional fluctuations in solvent loading or capture efficiency will be observed following a return  
 197 to baseload flow conditions, as observed by Tait et al. (2016)

- 198 2. The solvent becomes fully mixed within approx. 1.25 circulations of the entire solvent inventory.
- 199 3. The circulation time between desorber outlet and absorber inlet is less than 5min. Any changes in  
 200 solvent loading at the desorber outlet due to step-changes in reboiler heat input should induce a  
 201 CO<sub>2</sub> capture efficiency response within 5min.

202 As this test was carried out at a solvent flowrate of 1200l/hr and the eventual baseload condition has a flow  
 203 rate of 1000l/hr, a reasonable approximation is to multiply the circulation times obtained in this test by  
 204 1.2 to obtain circulation times at 1000l/hr (fig.5).  
 205



206  
 207  
 208

209  
 210 **Fig. 5. Important solvent circulation times for dynamic operation, scaled to 1000m<sup>3</sup>/hr**  
 211

212 These circulation tests provide a reasonable estimate of solvent circulation times, and are useful in the  
 213 planning of experiments and analysis of plant response early in the test campaign. However, as  
 214 demonstrated in section 5 it is possible to use online solvent sensors, plant temperatures and capture  
 215 efficiency to build on this initial analysis and construct a much clearer picture of plant response.  
 216

### 217 3.2 Baseload Operating Conditions

218 Due to changes in ambient conditions, general flow variability and varying nominal MEA concentration due  
 219 to water losses these baseload conditions should be regarded as approximate.  
 220

Controlled Variable	Value
Gas Flowrate at absorber inlet (Nm <sup>3</sup> /h)	200
Gas inlet temperature (°C)	42
Inlet gas CO <sub>2</sub> concentration (% v/v)	12
Pressurised hot water flow rate (m <sup>3</sup> /hr)	10
Solvent flowrate (l/h)	1000
Pressurised hot water inlet temperature (°C)	124
Pressurised hot water outlet temperature (°C)	118.5
Liquid inlet temperature, Absorber (°C)	40
Liquid inlet temperature, Desorber (°C)	98
<b>Measured Parameter</b>	
CO <sub>2</sub> capture efficiency (%)	91.5-95
Reboiler duty (GJ/tCO <sub>2</sub> )	6.2-6.8
L/G ratio (l/m <sup>3</sup> )	5.0
Nominal amine concentration (% w/w)	28-34
Rich Solvent Loading (mol CO <sub>2</sub> /mol amine)	0.36-0.40
Lean Solvent Loading (mol CO <sub>2</sub> /mol amine)	0.13-0.17



221 **Table 1. Baseload Operating Conditions**

222  
223 The baseload liquid-to-gas flow ratio (L/G) is established as 5 l/m<sup>3</sup>. The minimum solvent flow rate  
224 achievable without risking damage to solvent pumps is 400l/hr so a flow rate of 1000l/hr allows solvent  
225 flow to be reduced to 50% of its baseload value (500l/hr) while affording the operators a reasonable  
226 margin for error. The gas flow is operating close to its maximum for this plant at 200m<sup>3</sup>/hr.

227 It is worth noting that the baseload operating conditions reported here correspond to a necessary reference  
228 point, which allow for large changes in amplitude of key operating variables, such as solvent flowrate, gas  
229 flow rate, etc. It does not necessarily correspond to the optimised conditions for minimising reboiler duty.  
230 This is one reason explaining why the reboiler duty is higher than reported for other comparable facilities.  
231 The other reason is due to the small size of the cross-flow heat exchanger. In most CO<sub>2</sub> capture facilities the  
232 approach temperature for the cross-heat exchanger is approx. 10°C. For this pilot facility the process fluid  
233 (rich solvent) exits the heat exchanger at approx. 98°C while the working fluid (lean solvent) enters the  
234 heat exchanger at approx. 118°C, for an approach temperature of 20°C. A lower desorber inlet temperature  
235 requires more energy input from the reboiler as sensible heat to bring the incoming solvent up to stripping  
236 temperature. The additional contribution to the reboiler duty due to the undersized heat exchanger ( $\Delta Q_{reb}$ )  
237 can be calculated as follows.

$$\Delta Q_{reb} = \frac{m_{rich} C_{p_{rich}} \Delta T_a}{m_{CO_2}} \quad (\text{Equation 1})$$

238  
239 Where  $m_{rich}$  is the mass flow rate of rich solvent in kg/s,  $C_{p_{rich}}$  is the specific heat capacity of the rich solvent  
240 in J/kg.K,  $\Delta T_a$  is the difference in approach temperature between this facility and one with an optimised  
241 heat exchanger in K and  $m_{CO_2}$  is the CO<sub>2</sub> capture efficiency in kg/s. With  $\Delta T_a = 10K$  the additional  
242 contribution to the reboiler duty ranges between 1.033GJ/tCO<sub>2</sub> and 1.084GJ/tCO<sub>2</sub>, accounting for changes  
243 in capture efficiency and nominal MEA concentration (see table 1).

244 Due to water losses through the absorber and desorber gas outlets the nominal MEA concentration of the  
245 solvent increases over time. An automatic, batch-wise water topup system exists, but to avoid additional  
246 perturbations during dynamic testing it is not used over the duration of the test campaign. Instead, water  
247 levels are topped up in a single large batch at the start of each test day if MEA concentration becomes too  
248 high.

249 This variation in amine concentration appears to reduce the reboiler duty as the solvent becomes more  
250 concentrated in amine (see fig. 6). Increased amine concentration may also have the effect of lowering the  
251 lean and rich solvent CO<sub>2</sub> loading and increasing the capture efficiency. Although the volumetric flow of  
252 solvent remains constant, the molar flow rate of lean amine into the absorber increases thus decreasing the  
253 lean solvent CO<sub>2</sub> loading. Additionally, the baseload plant conditions are such that the solvent never  
254 reaches a saturated rich CO<sub>2</sub> loading (around 0.5 mol MEA/mol CO<sub>2</sub>), therefore a reduction in lean solvent  
255 CO<sub>2</sub> loading entering the absorber can also correspond to a reduction of rich solvent CO<sub>2</sub> loading leaving  
256 the absorber. The mass ratio of CO<sub>2</sub> in reaction products to H<sub>2</sub>O in the rich solvent is increased, reducing  
257 the energy lost into the water as sensible or latent heat per mole of CO<sub>2</sub> liberated. Finally, leaner solvent  
258 entering the absorber results in a larger driving force for CO<sub>2</sub> absorption and therefore a higher capture  
259 efficiency.

260

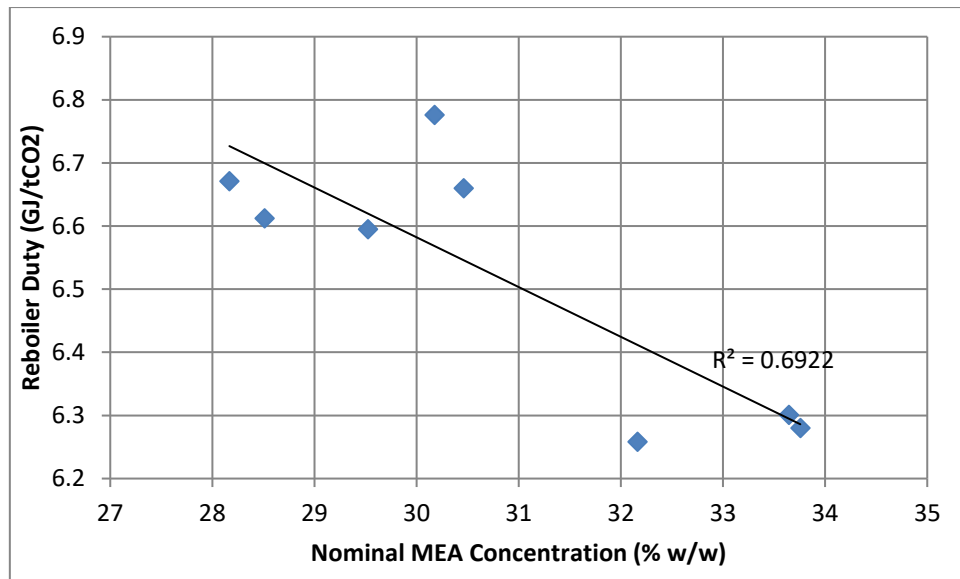


Fig. 6 Reboiler Duty Variance with amine concentration

261  
262  
263  
264  
265  
266  
267  
268  
269  
270

Figure 6 shows how the reboiler duty appears to decrease with nominal amine concentration at steady-state, baseload flow conditions. To minimise uncertainty due to short-term variations in temperature, capture efficiency and flow, the reboiler duties are calculated using the average hot water inlet/outlet temperature, CO<sub>2</sub> capture efficiency and hot water flow rate over a 20 minute period. The nominal amine concentration is the average of four measurements (2x lean, 2x rich) taken at the beginning and end of this 20 minute period.

### 3.2.1 Titration measurements and uncertainty

271  
272  
273  
274  
275  
276  
277  
278  
279  
280  
281  
282  
283  
284  
285  
286

Lean and rich solvent samples are taken at regular intervals during dynamic testing and analysed for MEA and CO<sub>2</sub> content using a Mettler Toledo T90 auto-titrator. Determination of CO<sub>2</sub> concentration in amine solvents using MEA is well-established, and is first described by Wonder et al. (1959). Samples were titrated against 0.2M HCl to determine total amine concentration, then 0.5M NaOH to determine CO<sub>2</sub> concentration. The titration method measures the total concentration of free amine and CO<sub>2</sub> in each sample. These measurements are then used to calculate the nominal amine concentration, which neglects the mass of CO<sub>2</sub> in the sample to determine the mass ratio of free amine to water. This is a useful measurement to make as the concentration of CO<sub>2</sub> in samples varies depending on operating conditions, and the nominal concentration indicates if the solvent has degraded from its optimal value (in the case of MEA, 30% by mass).

To determine the uncertainty of titration measurements a solution of 29.40%wt MEA (nominal) and 8.04%wt CO<sub>2</sub> equivalent is made up gravimetrically by bubbling CO<sub>2</sub> through MEA solution in a dreschel flask. The loaded solution is titrated for MEA and CO<sub>2</sub> content in triplicate. The uncertainty in bench CO<sub>2</sub> loading measurements is found to be +/- 3.15% relative, summarised in table 2.

MEA concentration (% wt, via titration)	CO <sub>2</sub> concentration (%wt, via titration)	MEA concentration (% wt nominal, calculated)	CO <sub>2</sub> loading (mol CO <sub>2</sub> /mol MEA, calculated)
27.068	7.876	29.38	0.403
26.942	7.936	29.26	0.409
27.307	7.751	29.60	0.395

Table 2. Titration measurements for determination of uncertainty

287  
288  
289  
290

291 **3.2.2 Online solvent sensors**

292 Two online solvent composition sensors are located in the lean and rich solvent lines (see fig. 1). In-situ  
293 measurements of solvent physical properties are used to determine amine concentration and CO<sub>2</sub> loading  
294 in real-time. The sensor used by Tait et al. (2016) is modified to comply with site safety regulations and to  
295 add remote operation capability. It was deployed along with a second device which has the same design. A  
296 detailed account of sensor development is provided by Buschle (2015). The specifics of the method by  
297 which the sensor operates are currently restricted as the University of Edinburgh is in the process of  
298 commercialising the technology, but it operates on similar principles to others which can be found in the  
299 literature (example: van Eckeveld et al., 2014). Continuous rich solvent measurements are provided for 8  
300 of 9 dynamic scenarios and continuous lean solvent measurements for 7 of 9.

301

302 **3.3 Selection of dynamic scenarios**

303 Dynamic operations are selected to be representative of scenarios which may be encountered during the  
304 operation of a supercritical coal power unit fitted with post-combustion capture.

305

306 **3.3.1 Generation plant shutdown**

307 This scenario is designed to be a realistic representation of how a post-combustion capture plant would  
308 respond to generation plant shutdown, with flue gas and regeneration “steam” (in this case pressurised hot  
309 water) ramp rates based on real operating procedures for supercritical coal units with stated power  
310 outputs of 500 MW or greater (NETL, 2014). In this scenario and all others, flue gas flow is approximated  
311 as being proportional to generation plant output. Flue gas flow is ramped down until it reaches 30% of  
312 baseload, which is defined as minimum stable generation (MSG). Below MSG the flue gas contains too many  
313 impurities due to incomplete combustion (DECC and Parsons Brinckerhoff, 2014), so to avoid polluting the  
314 solvent the gas flow is reduced to zero at this time. Hot water (i.e. “steam”) is fed to the reboiler for as long  
315 as possible so the solvent is lean in preparation for startup. Once gas flow reaches zero, solvent flow is  
316 reduced to 50% of baseload and for practical reasons is allowed to circulate until rich and lean loading have  
317 converged, simulating a scenario in which solvent flow is left running overnight to make use of the plant  
318 site’s cooling water. A similar shutdown procedure is described in Ceccarelli et al. (2014) as applied to PCC  
319 on NGCC plant – in this case it is applied to coal. The comparative benefits of continuing to circulate solvent  
320 overnight as opposed to immediate shutdown as soon as the flue gas flow has stopped are discussed in  
321 section 4.1.1 The shutdown method has a direct impact on capture plant response on the next startup. Two  
322 plant startup methods were investigated, both of which were preceded by this method of shutdown.

323

324 **3.3.2 Generation plant startup 1**

325 Ramp rates for plant startup are taken from PACE (2014), with minimum stable generation defined as 30%  
326 of baseload. Two startup scenarios are simulated, both preceded by the shutdown method described in  
327 3.3.1 and intended to simulate a “hot start” of a coal plant, in which the plant is shut down in response to  
328 falling demand (DECC and Parsons Brinckerhoff, 2014). The first startup scenario simulates a situation in  
329 which the low-pressure steam turbine is allowed to reach full load before any steam is introduced to the  
330 reboiler. This results in an extended period during which the CO<sub>2</sub> capture efficiency is low and the plant  
331 requires several hours to reach the desired capture efficiency.

332

333 **3.3.3 Generation plant startup 2**

334 In the second startup scenario steam (i.e. hot water) is introduced to the reboiler as soon as it becomes  
335 available, resulting in a smaller drop in capture efficiency and the plant reaching steady state more rapidly.  
336 This kind of operating mode may be useful in cases where there are restrictive laws on large, short-term  
337 spikes in CO<sub>2</sub> emissions from point sources. This may also be a more cost effective start-up method at very  
338 high carbon prices.

339

340 **3.3.4 Frequency response via pressurised hot water flow reduction**

341 A coal power station which is equipped with post-combustion capture can provide additional flexibility in  
342 output via manipulation of the steam flow to the reboiler (Lucquiaud, 2009; Haines, 2014). In this scenario

343 the flow of hot water to the reboiler is reduced to 50% of baseload as the other 50% is redirected to the LP  
344 steam turbine. In a power plant equipped with PCC this would result in a rapid, but marginal increase in  
345 plant output which would allow the coal plant to be used in grid balancing operations such as frequency  
346 response. After the hot water flow has been at 50% of baseload for 2 hours it is ramped back up to baseload.

347

### 348 **3.3.5 Capture bypass via pressurised hot water flow decoupling**

349 This scenario simulates the plant operator taking actions at the capture plant level in order to maximise  
350 electricity power output and capitalise on high electricity selling price. Two capture bypass scenarios are  
351 implemented – Bypass scenario 1 maintains both solvent and gas flow rates at baseload while reducing the  
352 hot water flow rate to zero. Bypass scenario 2 maintains gas flow rate at baseload, but reduces the solvent  
353 flow to 50% of baseload while reducing the hot water flow rate to zero. This is to reduce the power  
354 consumption of the pumps, and to reduce the power consumption of the flue gas booster fan via  
355 minimisation of absorber pressure drop. The period of this event lasts 2 hours.

356

### 357 **3.3.6 Capture plant ramping**

358 This scenario simulates the operation of a load-following plant, which is identified as one of the five typical  
359 modes of operation for coal-fired power stations in the UK as of 2012 (Mac Dowell and Shah, 2015). The  
360 generation plant ramps down its output from 100% of baseload to 70% for a period of 2 hours, then ramps  
361 back up. Hot water flow and solvent flow are matched as closely as possible to the gas flowrate to maintain  
362 the baseload L/G flow ratio, and to maintain consistency with the conclusion of Mac Dowell and Shah  
363 (2015) that less steam is available for solvent regeneration during these events.

364

### 365 **3.3.7 Capture efficiency control using online solvent measurements**

366 Future advanced control systems for both coal and gas CCS plants are likely to require real-time  
367 measurements of solvent composition to anticipate changes in capture efficiency and respond in a manner  
368 which is optimised in terms of environmental, economic and operational boundaries (Luu, 2015). For  
369 example, there could be a situation in which the operator wishes to maximise revenue by providing an  
370 ancillary service such as fast reserve balancing by reducing the level of steam abstraction to the reboiler,  
371 but at the same time wishes to minimise CO<sub>2</sub> emissions charges for the duration. Optimised capture plant  
372 operation in such a scenario is not possible without discrete knowledge of capture plant dynamics (process  
373 gain, dead time, time constants), so a simplified version is implemented.

374 This scenario envisions a situation in which the operator has to drive the CO<sub>2</sub> capture efficiency to 30% via  
375 a steam decoupling event and immediately return to the baseload capture efficiency of 90% or higher. With  
376 flue gas and solvent flow kept constant at baseload, the hot water flow to the reboiler is shut down. The  
377 lean solvent sensor is used in combination with knowledge of plant hydrodynamics and response times to  
378 predict when the flow of hot water must be turned back on to achieve a minimum capture efficiency of  
379 30%.

380

## 381 **4. Discussion of dynamic operating scenarios**

382 In this section, plant trends from the dynamic scenarios are discussed in detail. Rich and lean titration  
383 measurements are based on solvent samples taken from the absorber outlet and desorber outlet,  
384 respectively. At baseload conditions the circulation time from lean solvent sampling port to absorber inlet  
385 and rich solvent sampling port to desorber inlet is approximately 3 minutes. The circulation time between  
386 the lean solvent sensor and the absorber inlet is also around 3 minutes at baseload flow conditions.

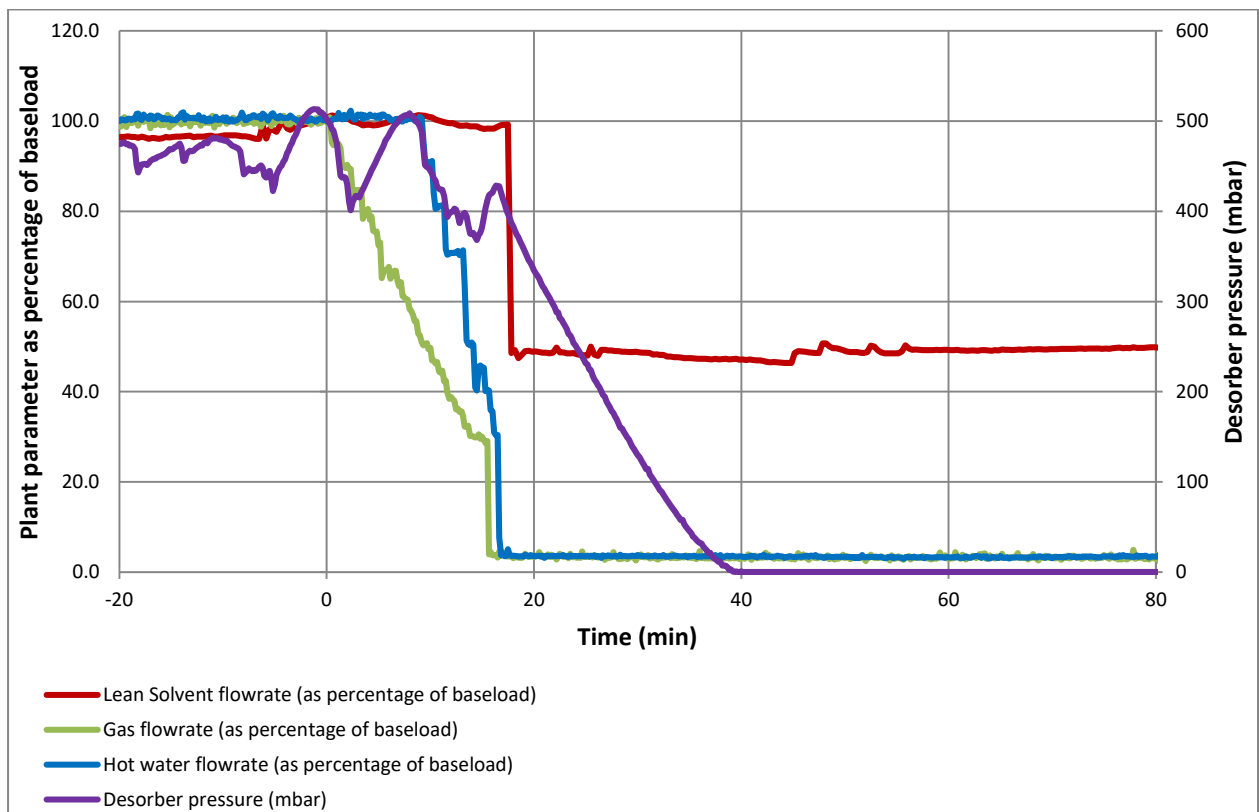
387

### 388 **4.1 Shutdown/Startup coupling 1**

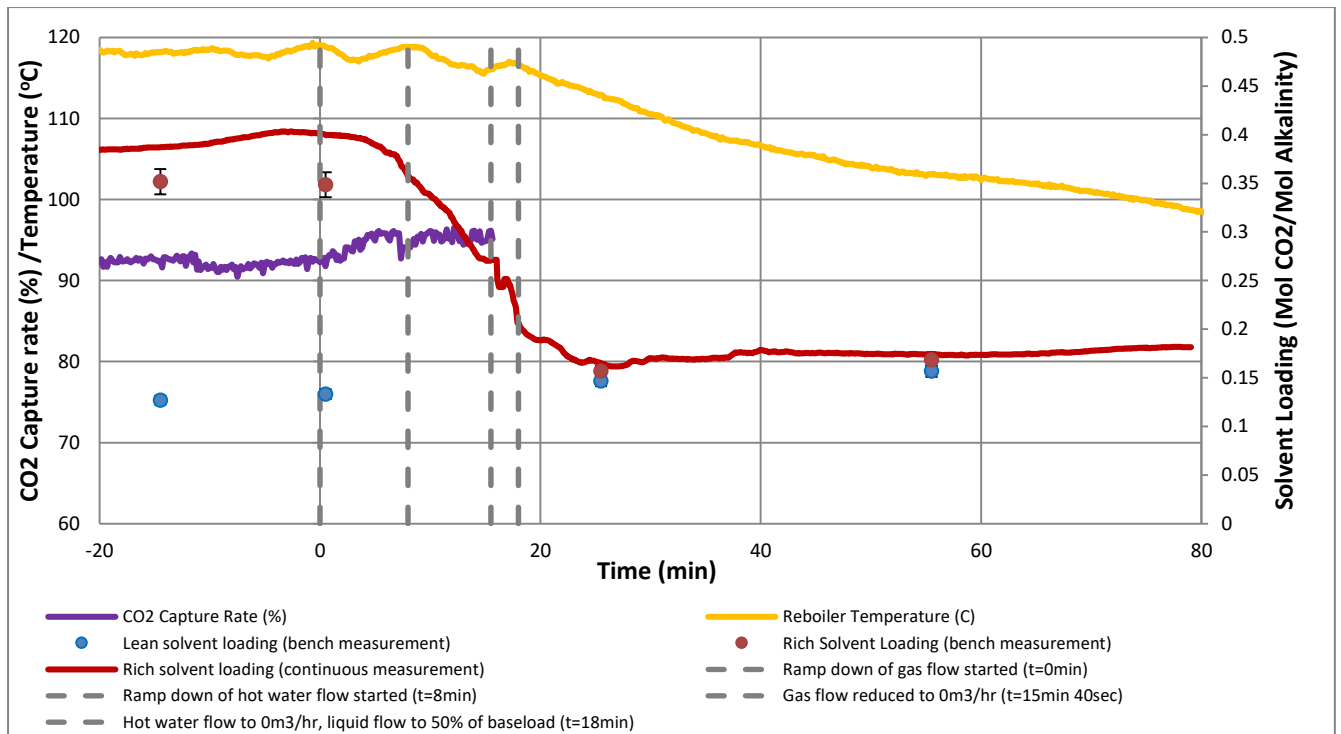
#### 389 **4.1.1 Shutdown**

390 Plant shutdown is initiated at t=0min (fig. 7a). Gas flow is ramped down at a rate of 5% of the baseload flow  
391 per minute (10 m<sup>3</sup>/hr) until it reaches 30% of baseload flow (60m<sup>3</sup>/hr), then reduced to zero. At t=9min,  
392 the flow of pressurised hot water to the reboiler is ramped down at a rate of around 10% of baseload per  
393 minute (1m<sup>3</sup>/hr) until it reaches zero at t=19min. The hot water flowmeter is unable to detect any flow  
394 below approx. 3m<sup>3</sup>/hr, accounting for the apparent immediate reduction of hot water flow to zero once it

395 reaches 30% of baseload at t=16min. The flow of hot water was controlled by the position of a proportional  
 396 solenoid valve, so it is assumed the hot water flow continued on a similar trajectory between t=16 mins  
 397 and t=19 mins. Once the flow of gas has been reduced to zero, solvent flow is reduced to 50% of baseload  
 398 (500kg/hr) and allowed to continue circulating until the reboiler has cooled to under 80°C and lean & rich  
 399 loadings have converged. This simulates the first part of a scenario in which the plant operator has allowed  
 400 the solvent inventory to continue circulating so that the plant is cool for the subsequent startup event. In  
 401 practice at a full-scale capture facility the operator may allow the solvent to continue circulating overnight,  
 402 making use of additional cooling to ensure the solvent is at ambient temperature for the subsequent startup  
 403 operation (Ceccarelli et al, 2014).  
 404 The CO<sub>2</sub> capture efficiency increases slightly over the course of the shutdown operation until the flow of  
 405 gas is switched off (fig. 7b). The gas flow rate is decreasing while the liquid flow rate remains constant,  
 406 resulting in a gradually increasing L/G ratio and higher capture efficiency. This also results in a decrease  
 407 in rich solvent CO<sub>2</sub> loading which, due to effective solvent mixing within the plant, rapidly converges with lean  
 408 loading and stabilises at around 0.18mol CO<sub>2</sub>/mol amine (fig. 7b). The volume of rich solvent contained in  
 409 the absorber sump is around 70l while the desorber contains around 400l of lean solvent, so the loading of  
 410 the fully mixed solvent inventory is closer to that of the lean. Continuous lean solvent measurement was  
 411 not available during this scenario.  
 412



413



414 **Fig. 7a. Gas, solvent hot water flow rate and desorber pressure as percentage of baseload operation,**  
 415 **shutdown scenario 1**

417 **Fig. 7b. Rich and lean solvent loading, reboiler temperature and CO<sub>2</sub> capture efficiency, shutdown**  
 418 **scenario 1**

419  
 420 The absorber temperature bulge decreases in magnitude and moves towards the base of the packed bed  
 421 over the course of the shutdown operation (fig. 8). The rate of CO<sub>2</sub> absorption per unit of column volume  
 422 decreases due to the decrease in gas flow rate, and a proportionally larger amount of CO<sub>2</sub> is absorbed close  
 423 to the gas inlet. Hot solvent holdup residing in the upper regions of the packed bed also flows down the  
 424 packing as time progresses, increasing the temperature closer to the base.  
 425  
 426

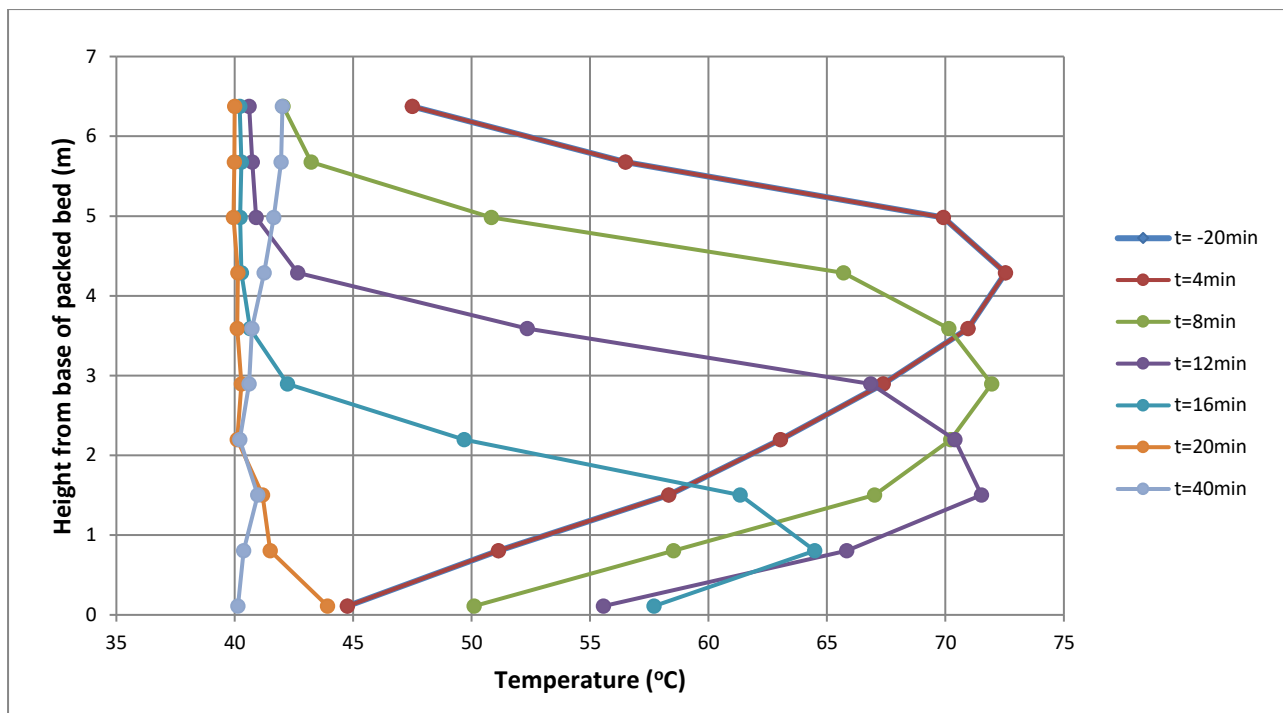


Fig. 8 Absorber temperature profile during plant shutdown scenario #1

427  
428  
429  
430

#### 4.1.2 Startup – standard procedure

431 This plant startup scenario intends to simulate a situation in which the low-pressure steam turbine  
432 achieves full power output before the introduction of steam to the reboiler. The startup procedure is based  
433 on real pulverised coal plant data (NETL, 2014). In anticipation of plant startup, the flow of solvent is  
434 stabilised at 50% of baseload. Titration measurements show that the lean and rich loadings are initially  
435 approx. 0.18 mol CO<sub>2</sub>/molamine. Gas is introduced to the absorber at t=0min (fig. 9a), when the  
436 hypothetical generation plant reaches minimum stable generation (30% of its stated power generation  
437 capacity). Once the gas flow is stabilised at 50% of baseload (100m<sup>3</sup>/hr) at t=20min, the solvent flow is  
438 increased to 100% of baseload (1000 l/hr) in anticipation of the next gas flow ramp, which is initiated at  
439 t=28min. Pressurised hot water is ramped at a rate of approx. 0.4m<sup>3</sup>/hr per minute from t=29min to  
440 t=54min. As mentioned previously, the hot water flow meter does not detect flow below around 30% of  
441 baseload (3m<sup>3</sup>/hr), but the hot water flow rate increase is assumed to have the same rate throughout the  
442 ramp. Hot water and gas flowrates both reach 100% of baseload at t=54min.

443 CO<sub>2</sub> capture efficiency is initially higher than at baseload due to the higher L/G ratio, but drops off rapidly  
444 at t=35min as lean loading at the absorber inlet rises (fig. 9b). At this time, lean solvent CO<sub>2</sub> loading at the  
445 absorber inlet becomes high enough to diminish the driving force for CO<sub>2</sub> absorption, reducing the capture  
446 efficiency. Solvent lean loading reaches a maximum at t=69min, while capture efficiency reaches a  
447 minimum at t=72min. If it is assumed that mixing effects in the pipework between the desorber sump outlet  
448 and absorber inlet are negligible, solvent which is analysed by the lean solvent sensor at t=x min will reach  
449 the absorber inlet at t=x+3 min.

450 Due to an error with the data-logging programme at t =200min, certain datasets after this time are  
451 unavailable. There is also a large spike in the rich solvent CO<sub>2</sub> loading online measurement at t=260-  
452 280min, but since the measured value exceeds 0.5mol/mol and a similar spike in titration measurements  
453 is not observed, this may be attributed to an instability of the rich loading sensor.  
454  
455

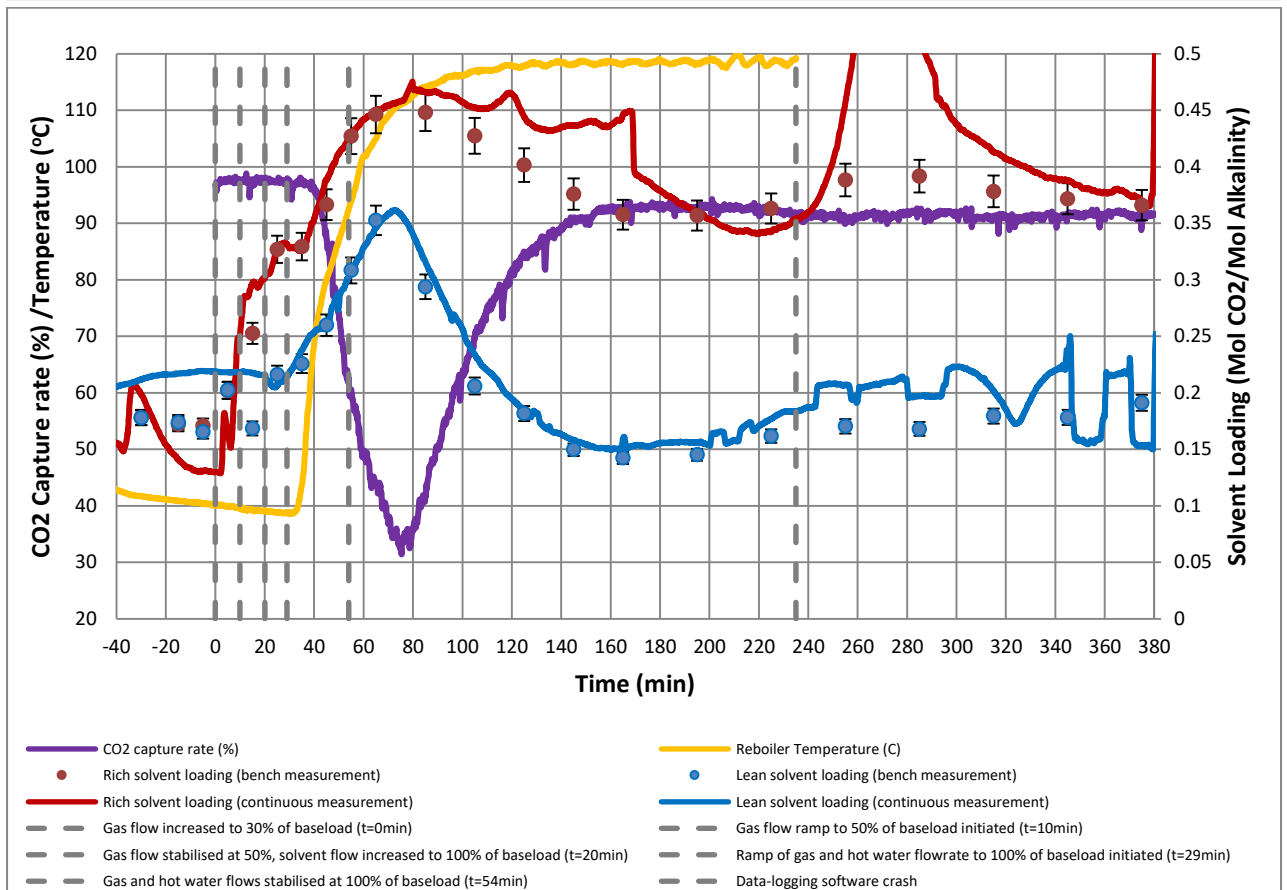
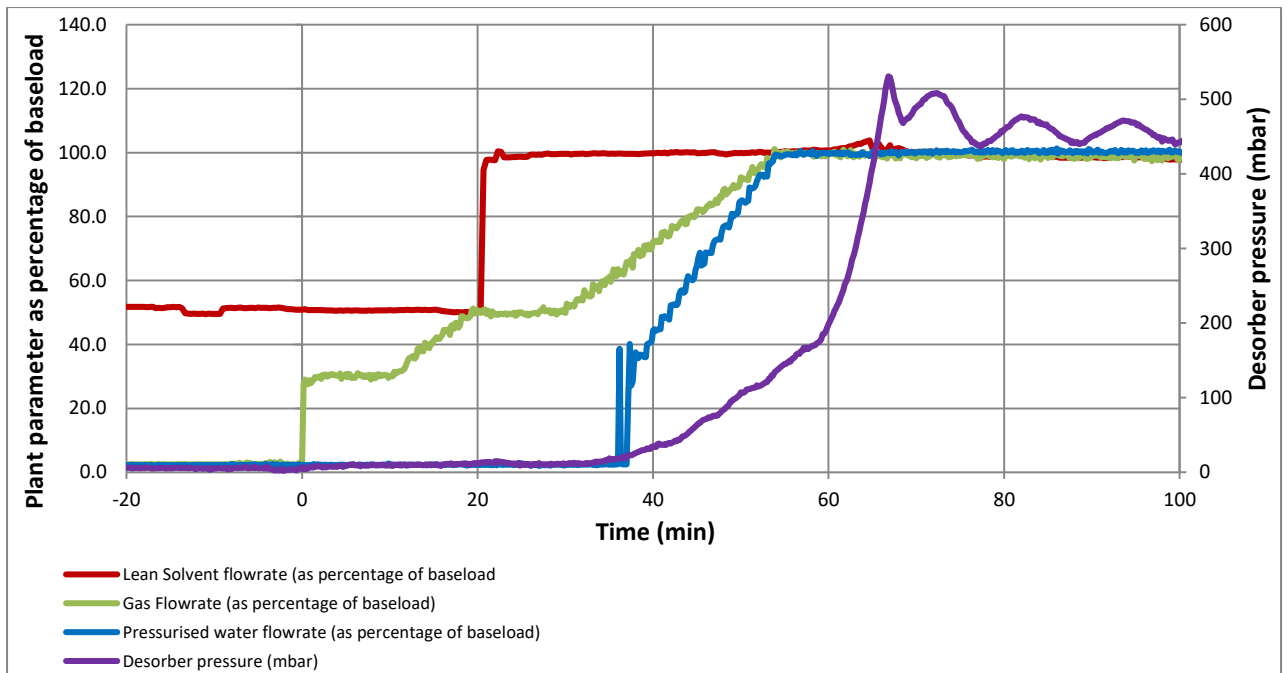
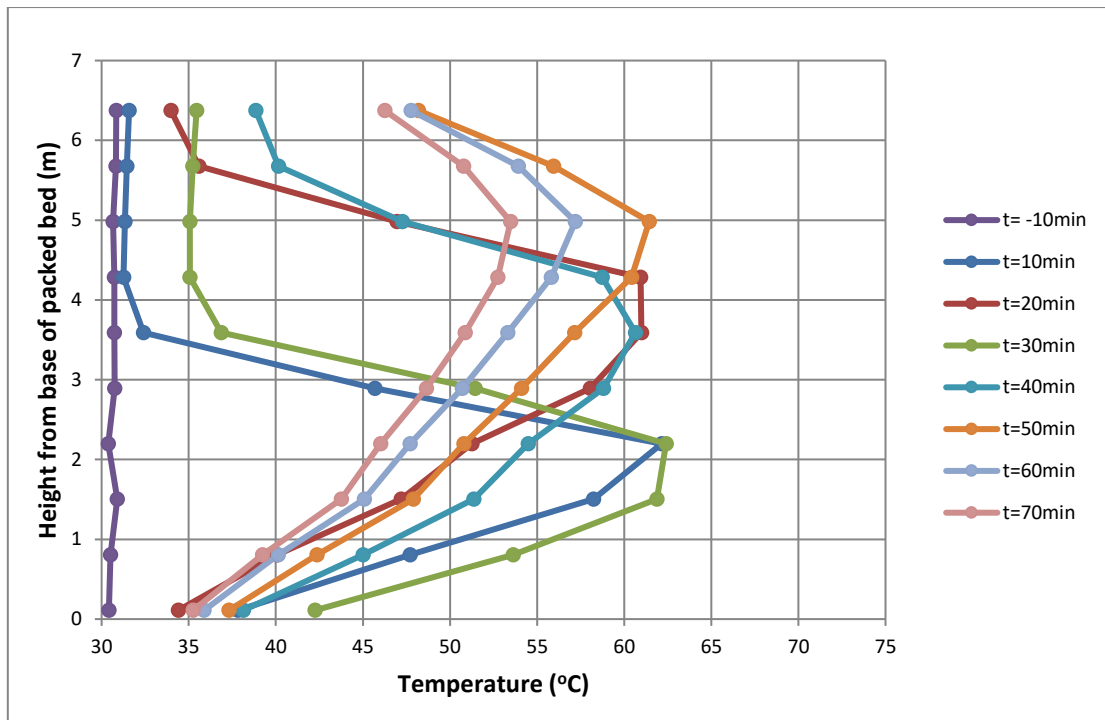


**Fig. 9a Gas, solvent hot water flow rate and desorber pressure as percentage of baseload operation, startup scenario 1**

**Fig. 9b Rich and lean solvent loading, reboiler temperature and CO<sub>2</sub> capture efficiency, startup scenario 1**





465

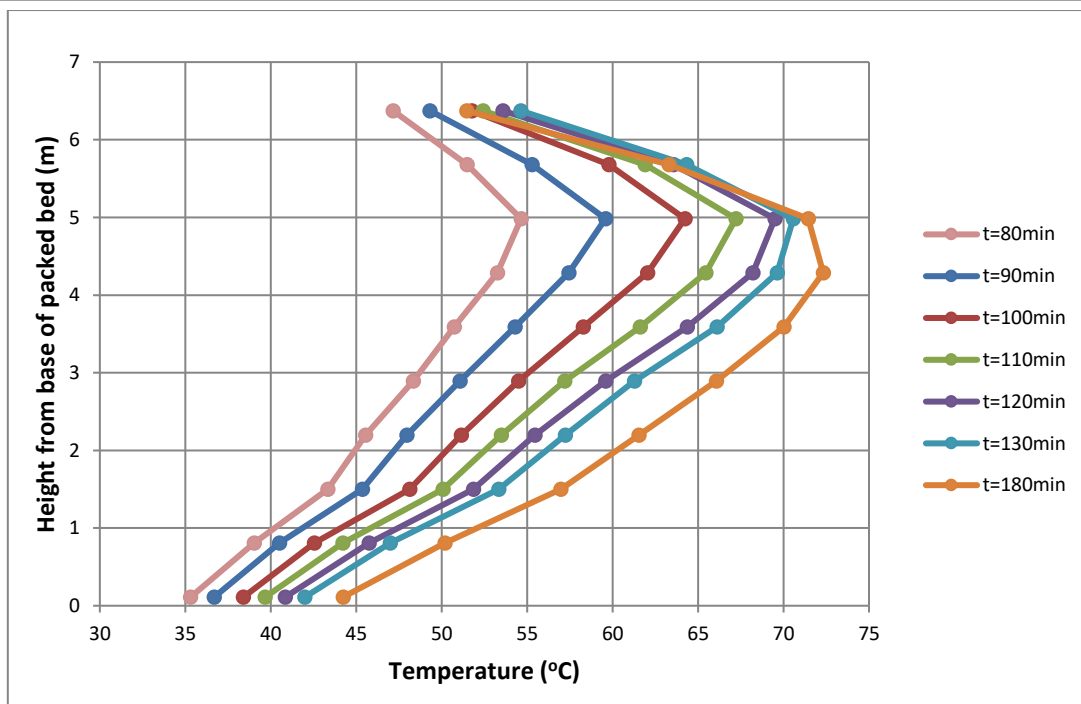


Fig. 10a Absorber temperature profile, startup scenario 1,  $t = -10\text{min}$  to  $t = 70\text{min}$

Fig. 10b Absorber temperature profile, startup scenario 1,  $t = 80\text{min}$  to  $t = 180\text{min}$

466

467

468

469

470

471

472

473

474

475

476

477

478

The absorber temperature bulge increases in magnitude and rises up the packed bed as the gas flow rate increases, until  $t=20\text{min}$  (fig. 10a). Just after  $t=20\text{min}$  there is a step-change in solvent flow rate from  $500\text{l/hr}$  to  $1000\text{l/hr}$ . This rapid increase in L/G ratio results in a larger proportion of the  $\text{CO}_2$  being absorbed close to the gas inlet, so the temperature bulge migrates to a lower location in the packed bed. As the flow of gas continues to increase, the L/G ratio decreases and the temperature bulge moves further up the packed bed. After  $t=50\text{min}$  it begins to decrease in magnitude as the lean loading at the absorber inlet increases and the capture efficiency falls. The observed increase in the lean loading during this period is due to lower rate of desorption. Although the flow rate of the pressurised hot water is being increased, the solvent temperature in the reboiler did not achieve the temperature high enough for stripping. Because of

479 the lower desorption rate, lean solvent leaving the reboiler and entering the absorber was at relatively  
480 higher lean loading which resulted in increased rich loading in the absorber and in return an increasing  
481 trend in lean loading until the reboiler temperature reaches operational temperature. At this point lean  
482 loading begins to decrease. Between  $t=70\text{min}$  and  $t=80\text{min}$  the capture efficiency begins to rise again, as  
483 does the magnitude of the temperature bulge until it is fully established at  $t=180\text{min}$  (fig. 10b).

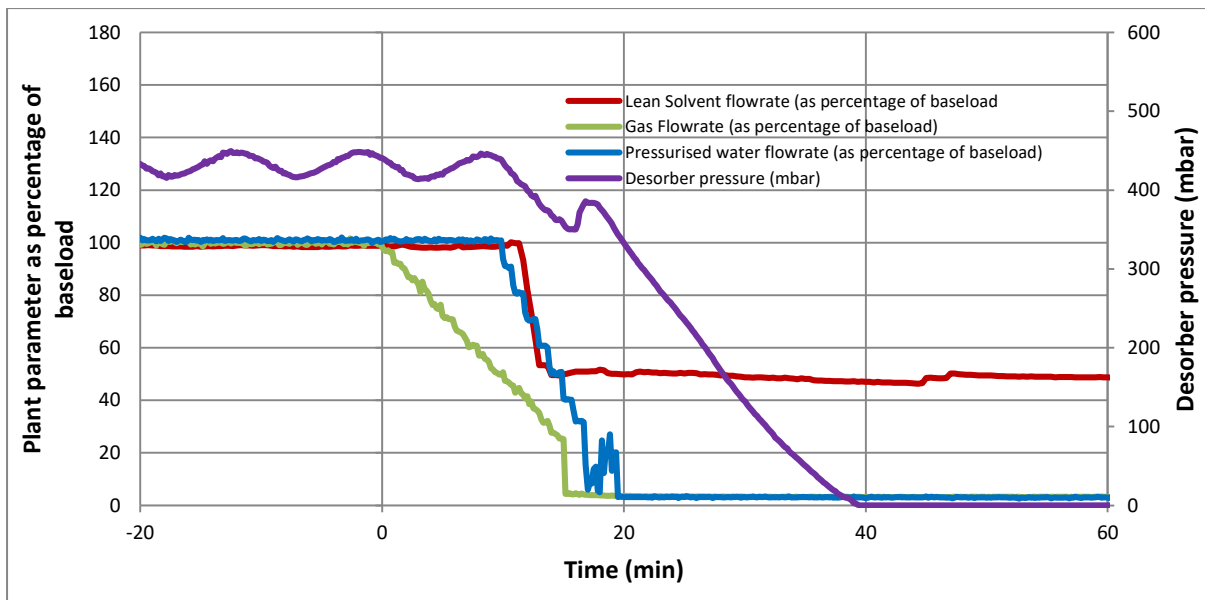
484  
485

## 4.2 Shutdown/Startup coupling 2

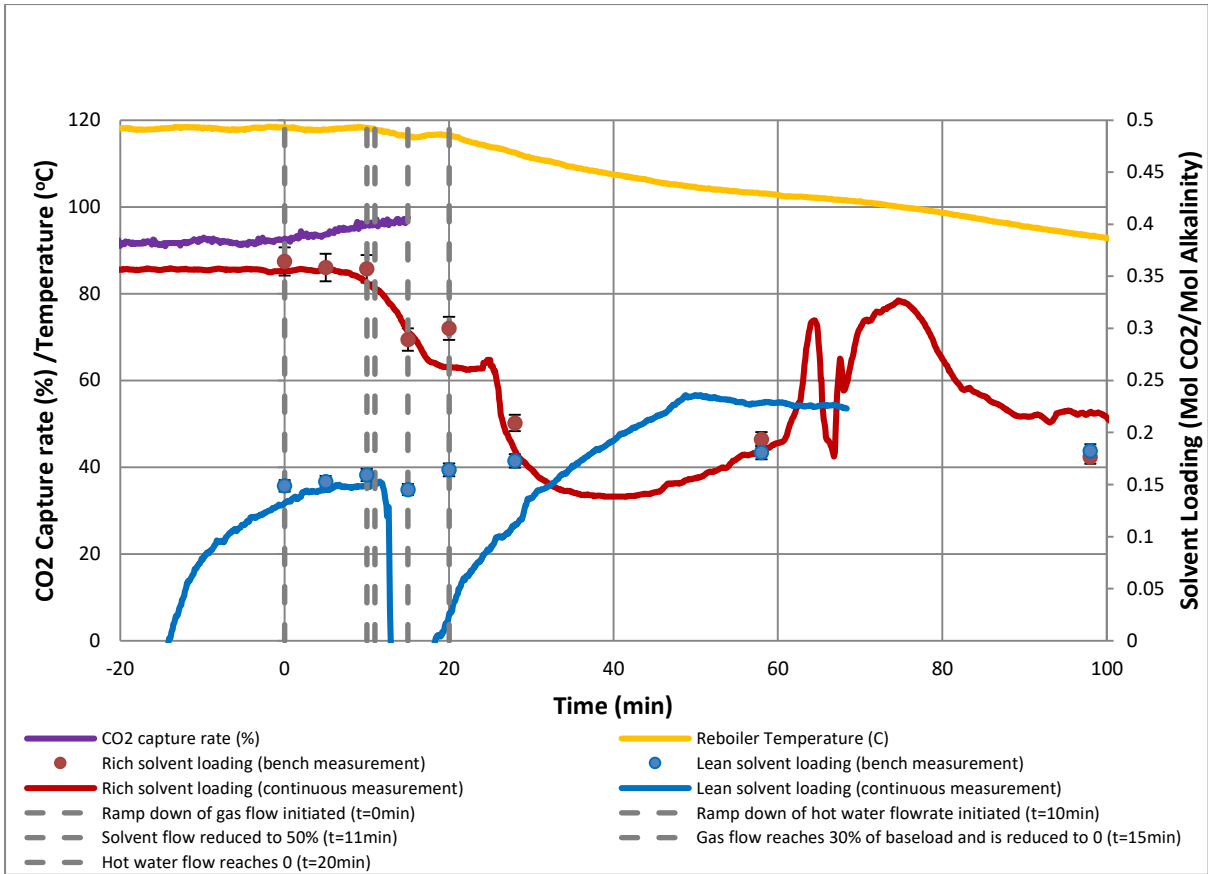
### 4.2.1 Shutdown

488 This shutdown scenario was carried out with similar changes in gas, liquid and hot water flow to shutdown  
489 scenario #1 (fig. 11a and 7a, respectively). Online lean and rich solvent sensors experienced stability issues  
490 prior to the initiation of this scenario. Therefore, manual solvent samples for off line analyses are taken at  
491 more regular intervals. This is to make sure that the effect of the shutdown operation on solvent loading  
492 can still be observed while online solvent measurements appear to be. A marginal increase is again  
493 observed in  $\text{CO}_2$  capture efficiency before the flow of gas is shut down, and rich & lean solvent loadings  
494 rapidly converge and stabilise at approx.  $0.18\text{ mol CO}_2/\text{mol amine}$  (fig. 11b). Temperature trends (fig. 11c)  
495 are similar to those of the previous shutdown operation (fig.8) with no significant differences.

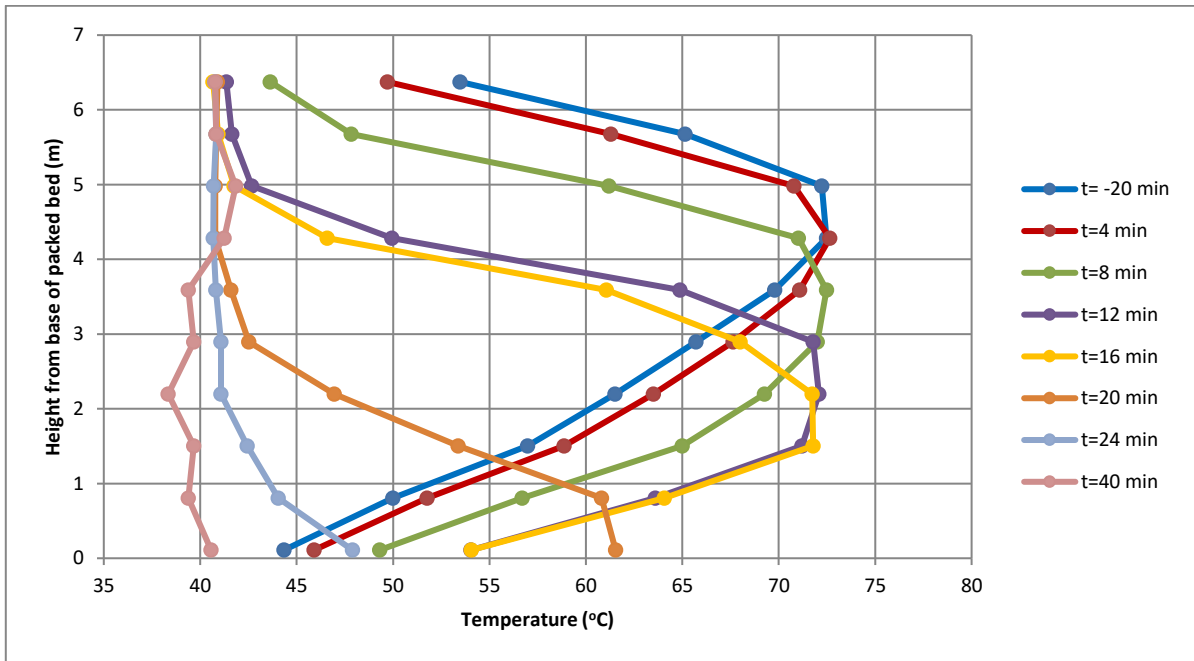
496



497



498



499  
500  
501  
502  
503  
504  
505  
506  
507  
508

Fig. 11a. Gas, solvent hot water flow rate and desorber pressure as percentage of baseload operation, shutdown scenario 2

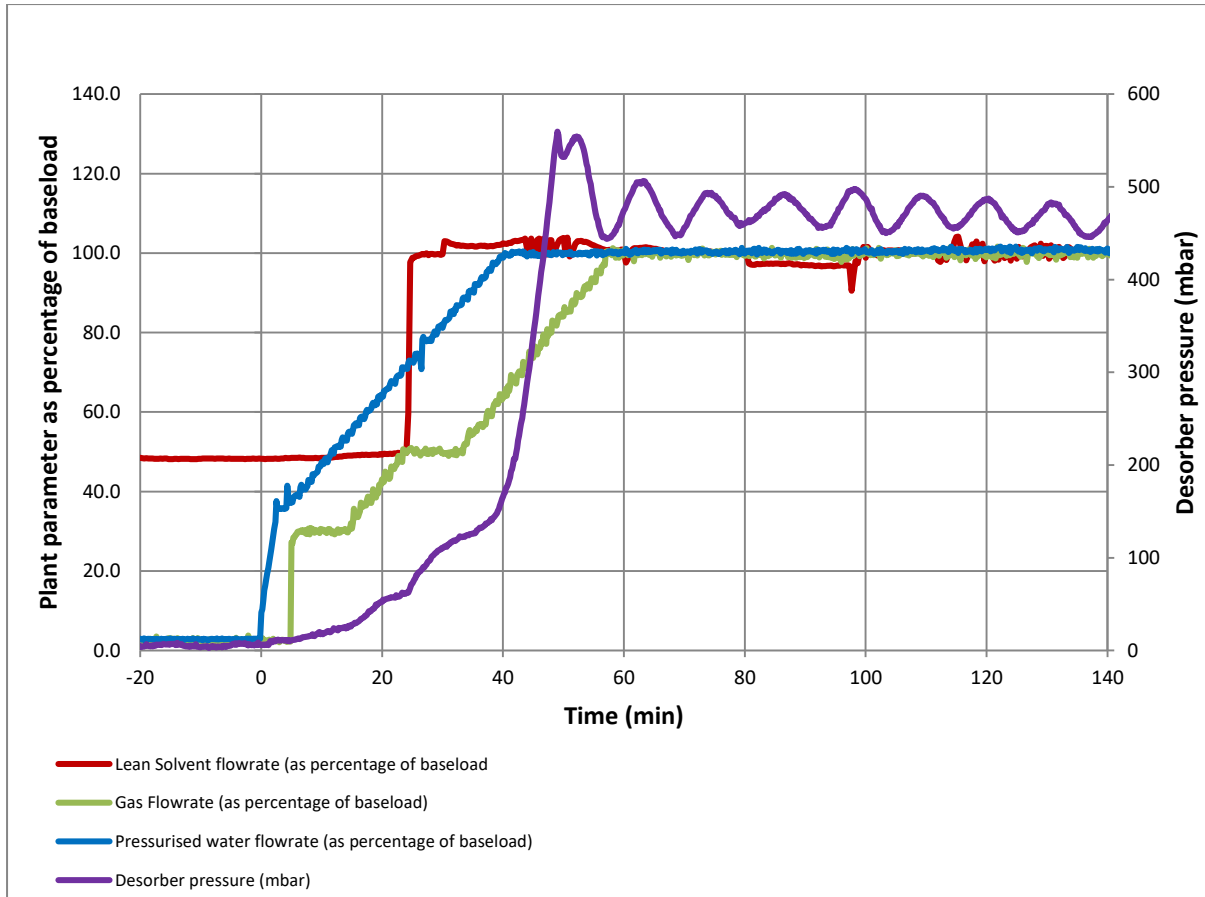
Fig. 11b. Rich and lean solvent loading, reboiler temperature and CO<sub>2</sub> capture efficiency, shutdown scenario 2

Fig. 11c Absorber temperature profile, startup scenario 2, t= -20min to t=40min

509 **4.2.2 Startup – with prioritisation of CO<sub>2</sub> emissions minimisation**

510 In this scenario steam is introduced to the reboiler as soon as it becomes available instead of after 35  
511 minutes, as was the case in the previous shutdown/startup coupling (section 4.1). This may be useful in  
512 situations where the plant operator is subject to significant emissions penalties in the case of large spikes  
513 in CO<sub>2</sub> emissions from a point source, or in the event of extremely high carbon price. Pressurised hot water  
514 is ramped up to 30% of baseload (3m<sup>3</sup>/hr) at t=0 and is subsequently ramped up at 1.75% of baseload  
515 (0.175m<sup>3</sup>/hr) per minute until it reaches 10m<sup>3</sup>/hr (fig. 12a). All other flow rates remain similar to the  
516 startup scenario described in section 4.1.2.

517



518

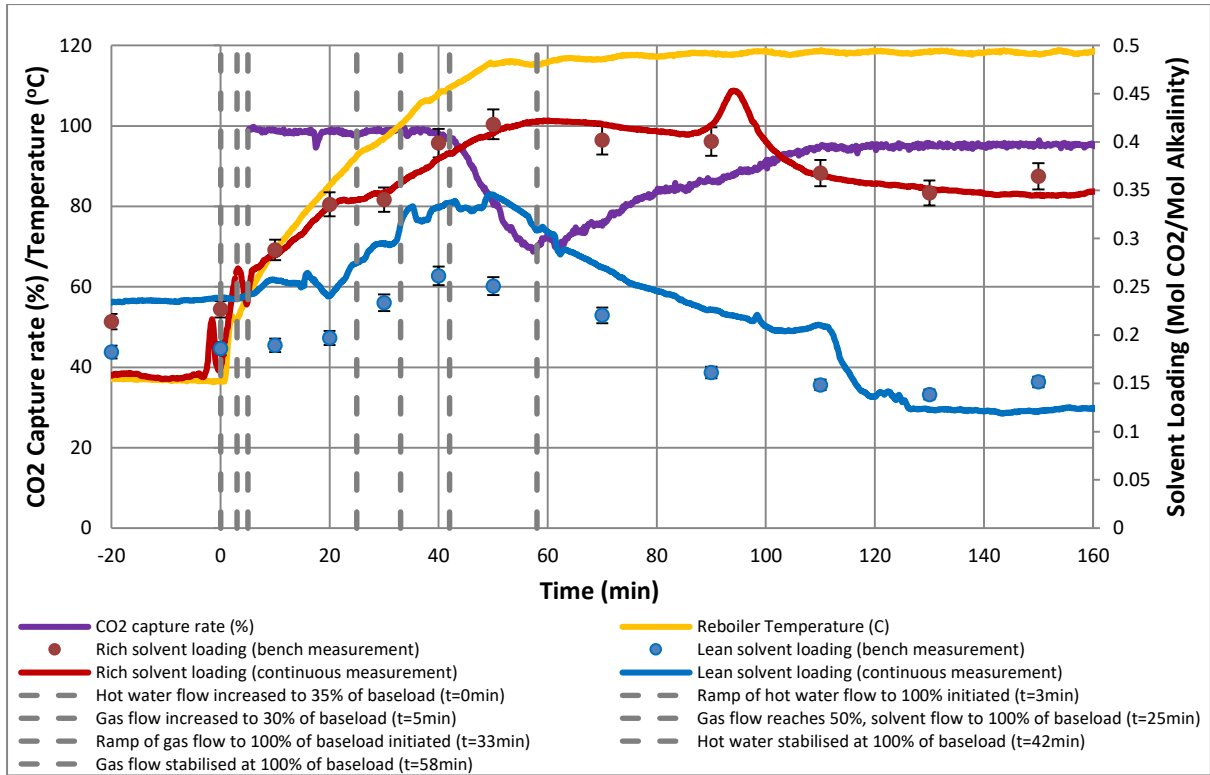


Fig. 12a. Gas, solvent hot water flow rate and desorber pressure as percentage of baseload operation, startup scenario 2

Fig. 12b. Rich and lean solvent loading, reboiler temperature and CO<sub>2</sub> capture efficiency, startup scenario 2

The reboiler reaches operational temperature much more rapidly than in scenario 4.1.2, so the drop-off in CO<sub>2</sub> capture efficiency is less sharp and reaches a minimum of approx 70% (fig. 12b) instead of 33%. If a similar approach were to be attempted during real plant startup operation, it could proceed by synchronising the turbine shaft while abstracting the maximum possible flow of steam from the IP/LP crossover, allowing the remainder to flow through the LP turbine to remove the resultant frictional heat. It may also be possible to extract additional steam from the HP turbine outlet during start-up, if maintaining a capture efficiency as close to 90% as possible were critical.

For comparison with the startup scenario described in 4.1.2 the total CO<sub>2</sub> emissions over the first 160mins of gas being introduced to the absorber are calculated. This length of time is selected as it is the duration required for the plant in scenario 4.1.2 to stabilise at baseload operating conditions (fig. 9b).

$$mCO_2 = \int_{0min}^{160min} \left( \frac{Q_{gas,t}}{60} \cdot \varphi_{CO_2,t} \cdot \rho_{CO_2,t} \right) \left( 1 - \frac{\eta_{CO_2,t}}{100} \right) \quad (\text{Equation 2})$$

$mCO_2$  is the total mass of CO<sub>2</sub> emitted,  $Q_{gas}$  is the volumetric flow rate of gas in m<sup>3</sup>/hr,  $\varphi_{CO_2}$  is the volume fraction of CO<sub>2</sub> in the gas phase,  $\rho_{CO_2}$  is the density of CO<sub>2</sub> at the gas inlet temperature and  $\eta_{CO_2}$  is the percentage CO<sub>2</sub> capture efficiency.  $mCO_2$  for startup scenario 4.1.2 is 25.1kg.  $mCO_2$  for startup scenario 4.2.2 is 10.3kg, a saving of 14.8kg CO<sub>2</sub> over the same time period.

To determine the potential effect on total daily CO<sub>2</sub> emissions this result is considered in the context of a coal-fired power station, equipped with CCS and operating under a two-shifting dispatch pattern. In this operating mode a hot startup is initiated at 6am, then operates at steady-state baseload with 90% capture efficiency until 10pm, for a total daily operating time of 16 hours.

Operating Scenario	Duration (mins)	Total startup CO <sub>2</sub> emissions (kg)	Total daily CO <sub>2</sub> emissions (kg)
--------------------	-----------------	--	--

Startup with prioritization of grid synchronization	160	25.1	79.4
Startup with prioritization of emissions minimization	160	10.3	64.6

**Table 3. Total CO<sub>2</sub> emissions in total kg per scenario**

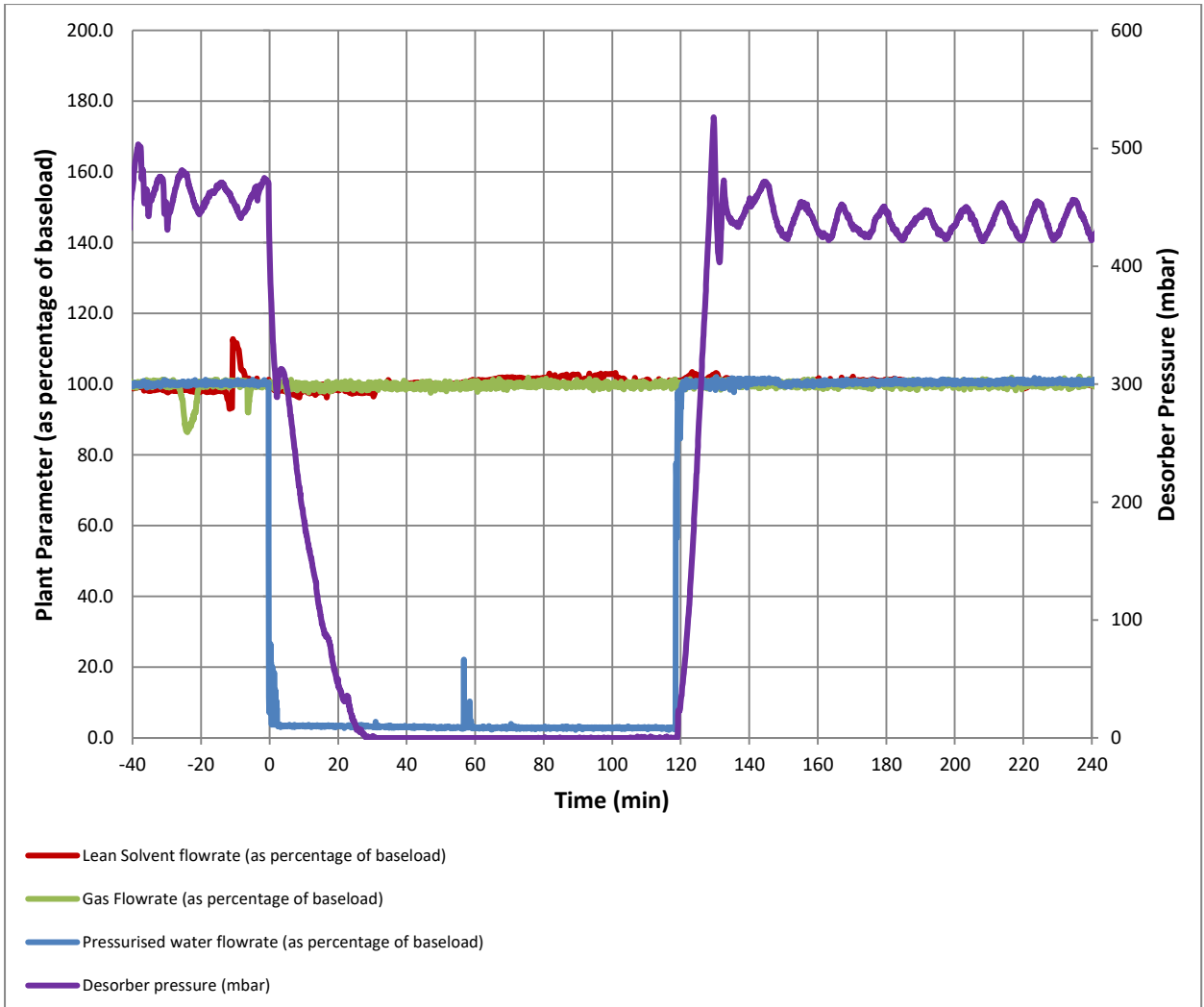
548  
549  
550  
551  
552  
553  
554  
555  
556  
557  
558  
559  
560  
561  
562  
563  
564  
565  
566  
567  
568  
569  
570  
571  
572  
573  
574

The saving of 14.8kg CO<sub>2</sub> during startup is approx. 18.6% of the total emissions for a day under two-shifting operation. As steam is introduced more rapidly in scenario 2 the total mass of steam used during the startup period increases by 23.6%. However, as stripping steam is extracted before the inlet of the low-pressure steam turbine the impact on overall plant energy output is likely to be small. Depending on the future emissions cost of CO<sub>2</sub>, this analysis shows that it may be economical to implement advanced control strategies to begin capturing CO<sub>2</sub> as rapidly as possible during a start-up event. A comparison of two similar scenarios at large-scale via, for example, dynamic modelling would be an interesting follow-up study.

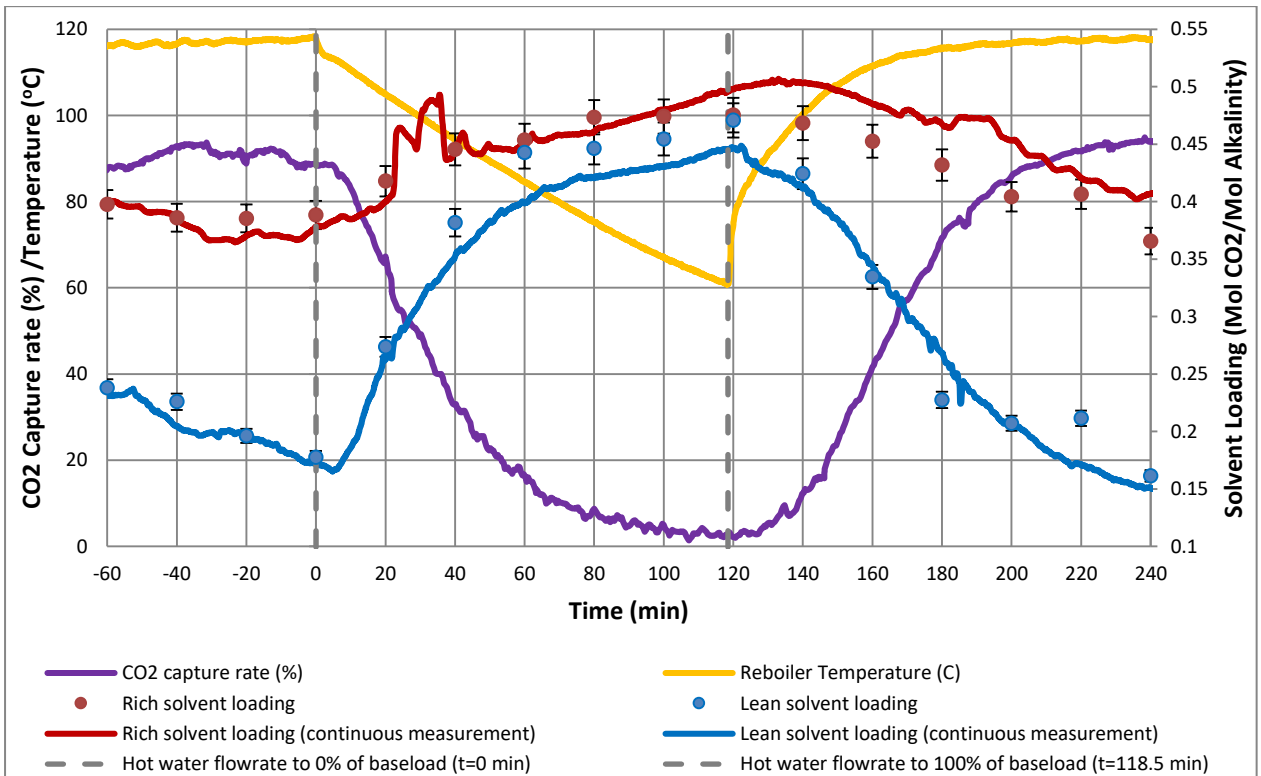
#### **4.3 Power output maximisation via hot water decoupling – Capture Bypass scenario 1**

It can be advantageous for plant operators to stop the flow of steam to the reboiler, redirecting it instead to the low-pressure steam turbine to capitalise on high electricity selling price. This scenario demonstrates how the capture plant responds to the decoupling of steam flow from the reboiler. It also provides valuable insights about plant circulation times and dynamics which prove useful for capture efficiency control using online solvent measurements (scenario 4.7).

Flow of hot water to the reboiler is switched off at t=0min (fig. 13a). The online solvent sensor detects a change in lean loading at t=5min, with the CO<sub>2</sub> capture efficiency responding at approximately t=8min (fig. 13b). The CO<sub>2</sub> capture efficiency decreases steadily as both rich and lean solvent become more concentrated in CO<sub>2</sub>. Hot water is reintroduced to the reboiler at t=118min 30sec. The lean solvent sensor detects a reduction in lean loading around 5mins after the step-change in reboiler heat input, at t=123min 30sec. The capture efficiency responds between t=126 and 127mins. The following conclusions can be drawn based on the observation made on the plant response time to introduction of step changes. If the plant is operating at baseload solvent flow conditions and a step change is introduced in hot water flow, a change in lean online solvent measurement appears after 5mins, and a change in capture efficiency appears after around 8mins (table 4).



575



576

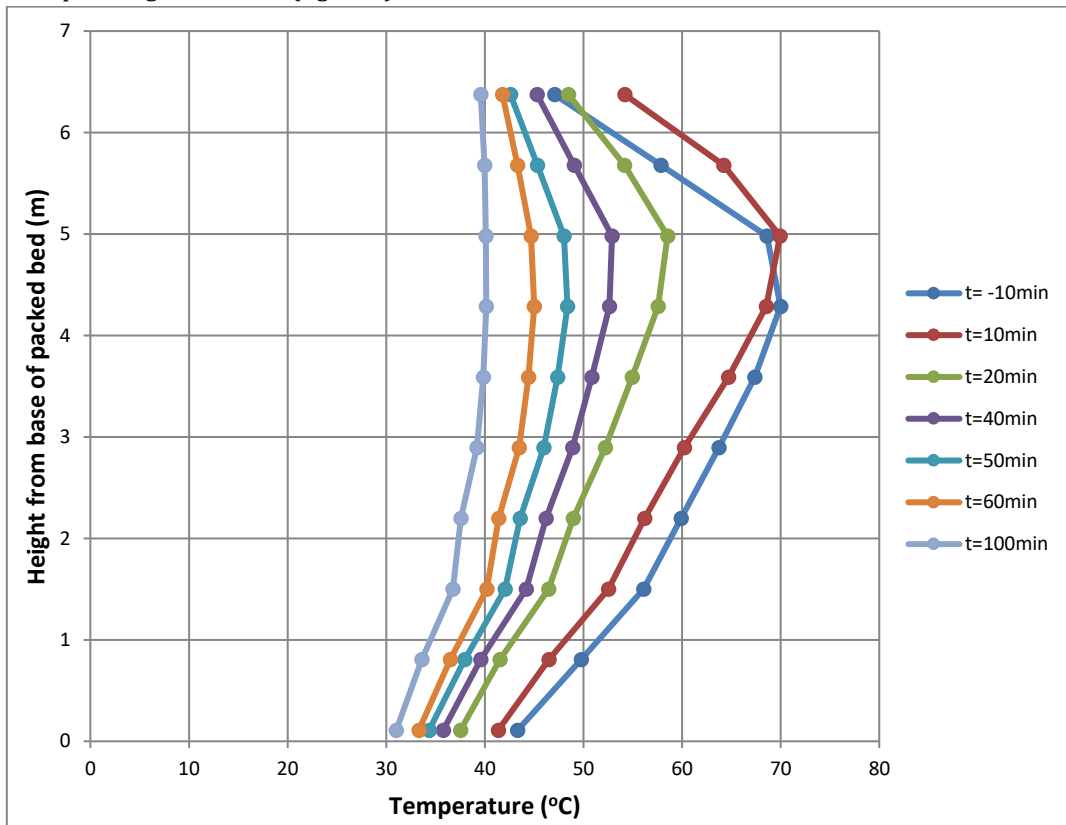
577 Fig. 13a. Gas, solvent hot water flow rate and desorber pressure as percentage of baseload operation,  
 578 capture bypass scenario 1

579 Fig. 13b. Rich and lean solvent loading, reboiler temperature and CO<sub>2</sub> capture efficiency, capture bypass  
 580 scenario 1  
 581

Event	Cause of event	Approximate elapsed time since hot water flow is reintroduced (min)
Hot water flow increased from 0m <sup>3</sup> /hr to 10m <sup>3</sup> /hr	Step-change in setpoint from operator.	0
Response in online lean loading measurement	Solvent which is leaner as a result of hot water step-change reaches the lean online solvent sensor.	5
Response in CO <sub>2</sub> capture efficiency	Leaner solvent reaches the absorber inlet.	8

582 **Table 4. Response of plant parameters to reintroduction of reboiler heat input**

583  
 584 The absorber temperature profile gradually decreases in magnitude along with the capture efficiency (fig.  
 585 14a). When the flow of hot water is reintroduced to the reboiler at 118min 30sec the capture efficiency  
 586 increases and the absorber temperature increases in magnitude until the plant reaches steady state,  
 587 baseload operating conditions (fig. 14b).



588



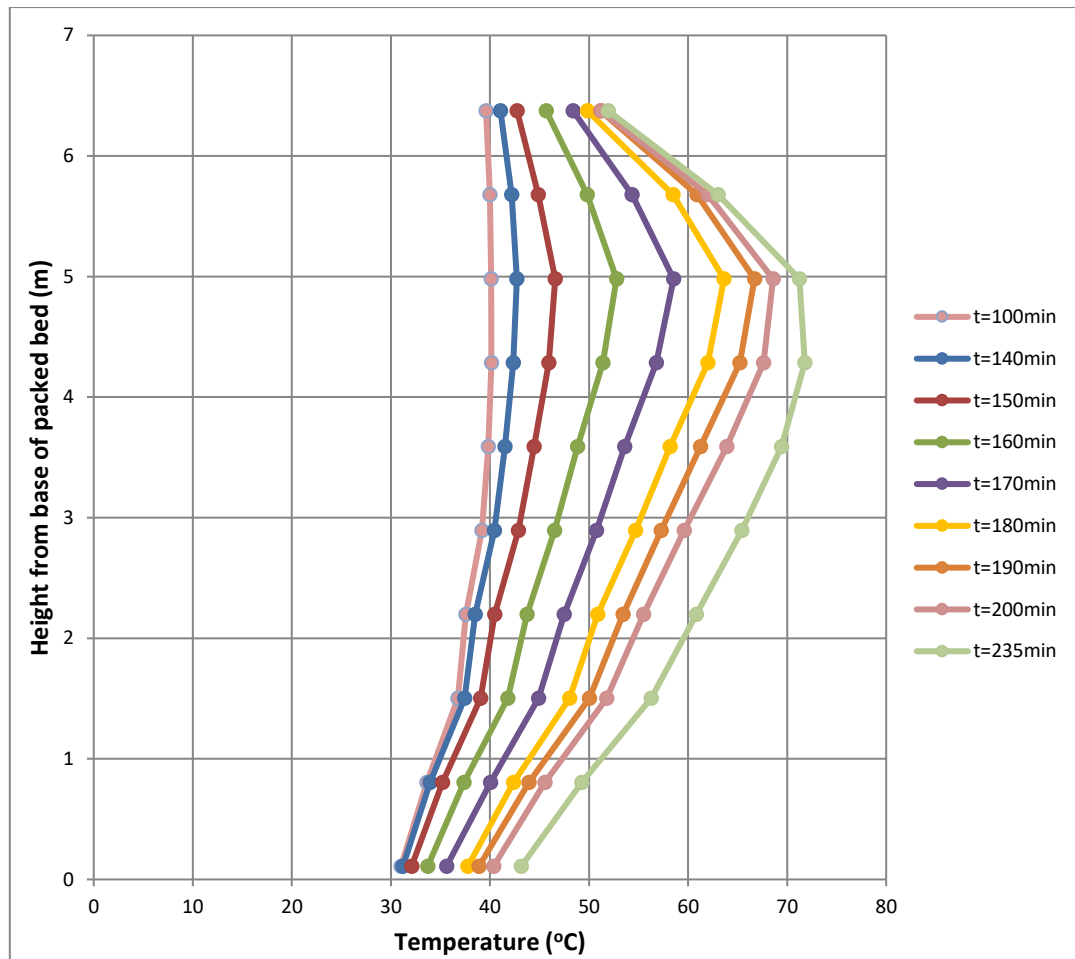


Fig. 14a. Absorber temperature profile, capture bypass scenario 1, t= -10min to t=100min

Fig. 14b. Absorber temperature profile, capture bypass scenario 1, t= 100min to t=235min

589

590

591

592

593

594

#### 4.4 Power output maximisation via hot water decoupling, solvent flow reduced by 50% - Capture bypass scenario 2

595

596

597

598

599

600

601

602

603

604

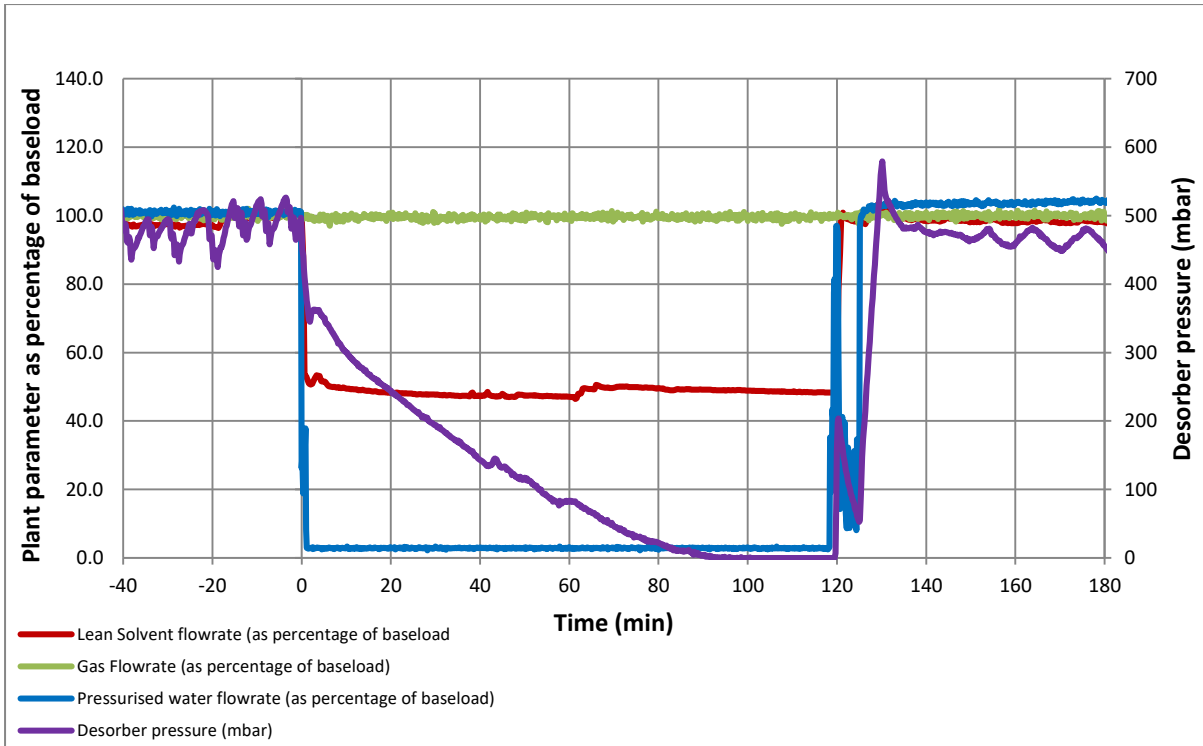
605

606

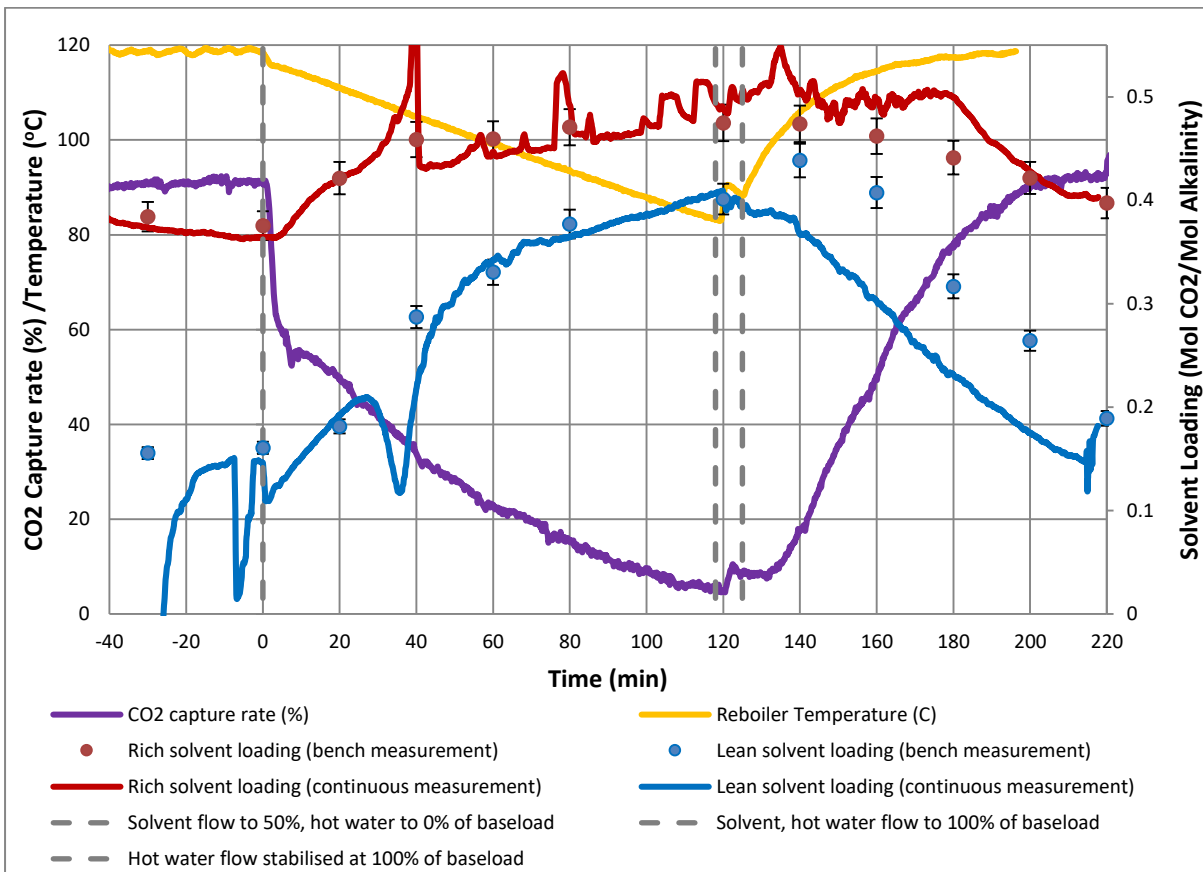
607

This scenario is similar to the previous hot water decoupling event (section 4.3), but the flow of solvent to the absorber is reduced to 50% in addition to the reduction of hot water flow to zero. In a real CO<sub>2</sub> capture plant, this would reduce both the power consumption of the pumps and the booster fan, via reduction of the pressure drop across the absorber.

Hot water flow to the reboiler is both reduced to zero and solvent flow is reduced to 50% of baseload at t=0min (fig. 15a). Due to the rapid decrease in L/G flow ratio the capture efficiency is reduced almost immediately, reaching 60% within 4 minutes (fig. 15b). Capture efficiency continues to decrease over the course of the hot water decoupling event. At t=118min the flow of solvent and hot water are both increased to 100% of baseload, but due to an error with the Labview control system the hot water flow is not stabilised at baseload until t=125min (fig. 15a). CO<sub>2</sub> capture efficiency begins to increase noticeably at around t=130mins, the plant response being slower than in scenario 4.3 due to the error with hot water flow stabilisation at t=118min.



608



609

610

611

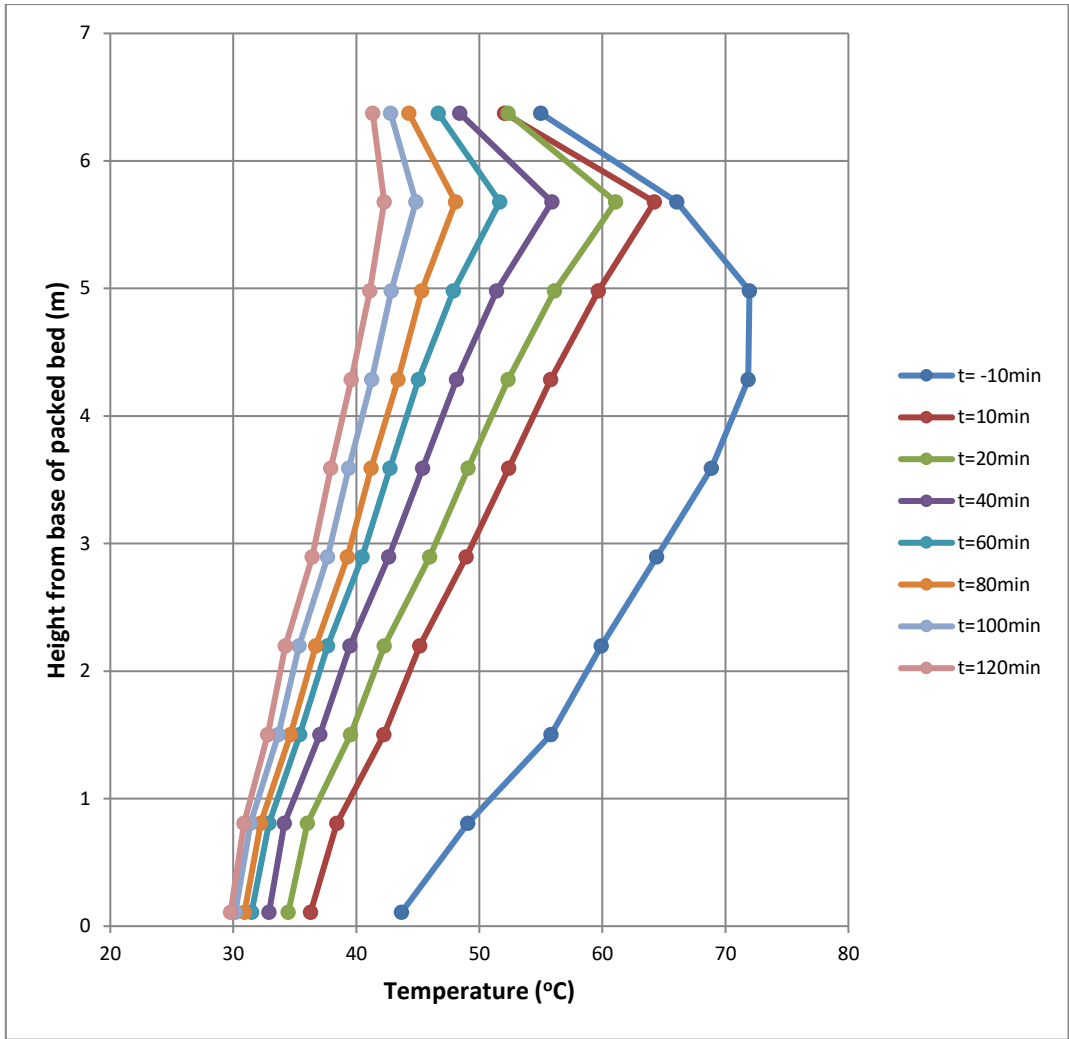
612

613

614

**Fig. 15a. Gas, solvent hot water flow rate and desorber pressure as percentage of baseload operation, power output maximisation event 2.**

**Fig. 15b. Rich and lean solvent loading, reboiler temperature and CO<sub>2</sub> capture efficiency, power output maximisation event 2**



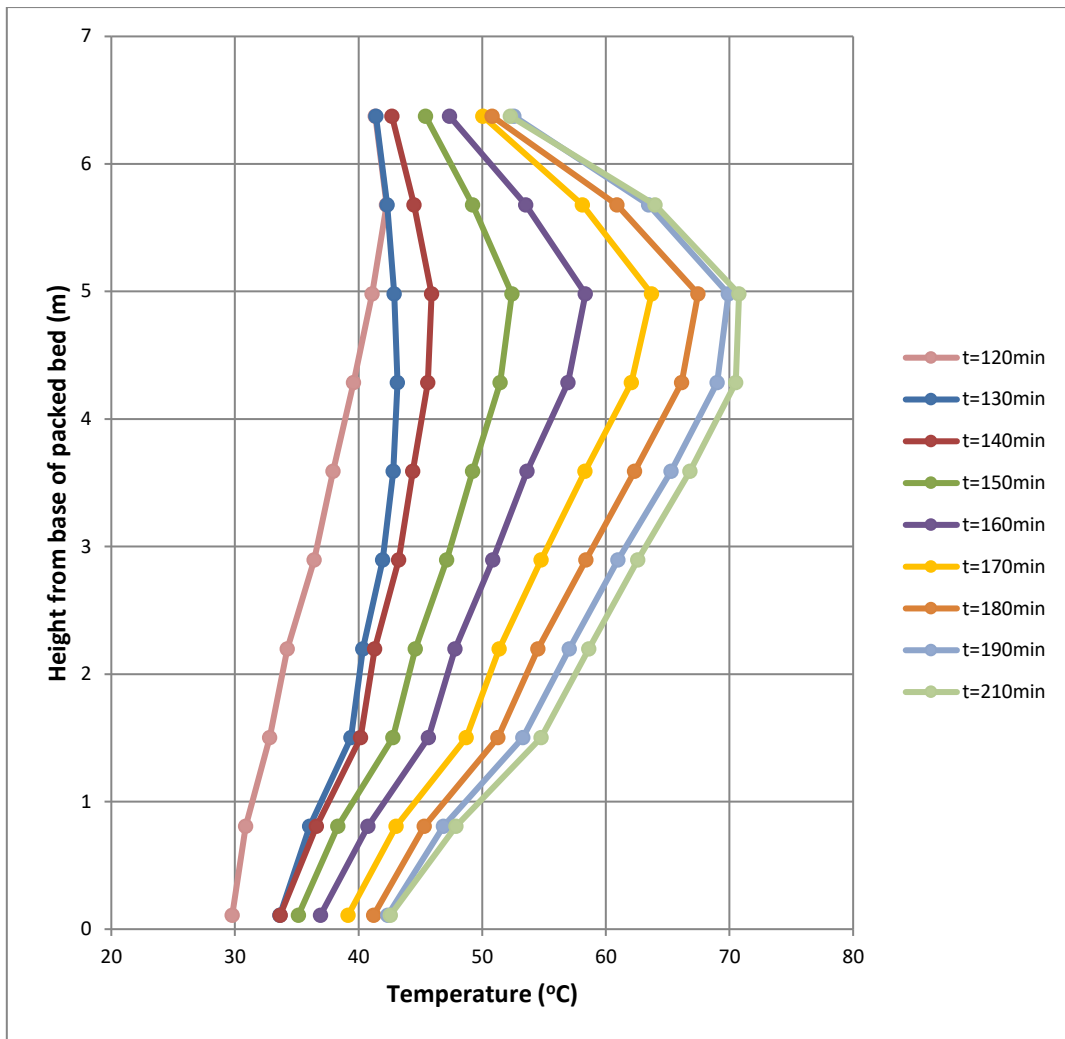


Fig. 16a. Absorber temperature profile, capture bypass scenario 2, t= -10min to t=120min  
 Fig. 16b. Absorber temperature profile, capture bypass scenario 2, t= 120min to t=210min

616  
 617  
 618  
 619

In comparison to the scenario 4.3 the absorber temperature profile follows a roughly similar trajectory although the initial decrease in the magnitude of the temperature bulge is more rapid due to the reduced solvent flow rate and hence, reduced capture efficiency (fig. 16a).

620

#### 4.5 Frequency response via hot water flow reduction

621

Coal-fired power stations can enhance their flexibility via the addition of post-combustion capture, which allows them to rapidly increase (or reduce) plant output via redirection of steam flow from the reboiler to the low pressure steam turbine (Lucquiaud, 2009; Haines and Davison, 2014). In this scenario the flow of hot water to the reboiler is reduced by 50% at t=0 (fig. 17a). All other plant flow rates remain at baseload throughout. A decrease in CO<sub>2</sub> capture efficiency is observed over the course of t=20min to t=100min, stabilising at around 75% (fig. 17b). This results in an 8°C decrease in absorber temperature bulge magnitude over this time period (fig. 18a).

622

At t=141min the flow of hot water to the reboiler is increased to 100% of baseload (fig. 17a). A response in capture efficiency is observed at approx. t=149min which is consistent with the plant response observed in scenario 4.3. The capture efficiency requires 70mins to increase to its original value, stabilising at around 93% at t=210min. The absorber temperature bulge increases to its original magnitude as the capture efficiency increases (fig. 18b).

623

The rich solvent online measurement is in close agreement with bench titration measurements, but the lean online measurement suffers from severe measurement instability until approx. t=122min.

624

625

626

627

628

629

630

631

632

633

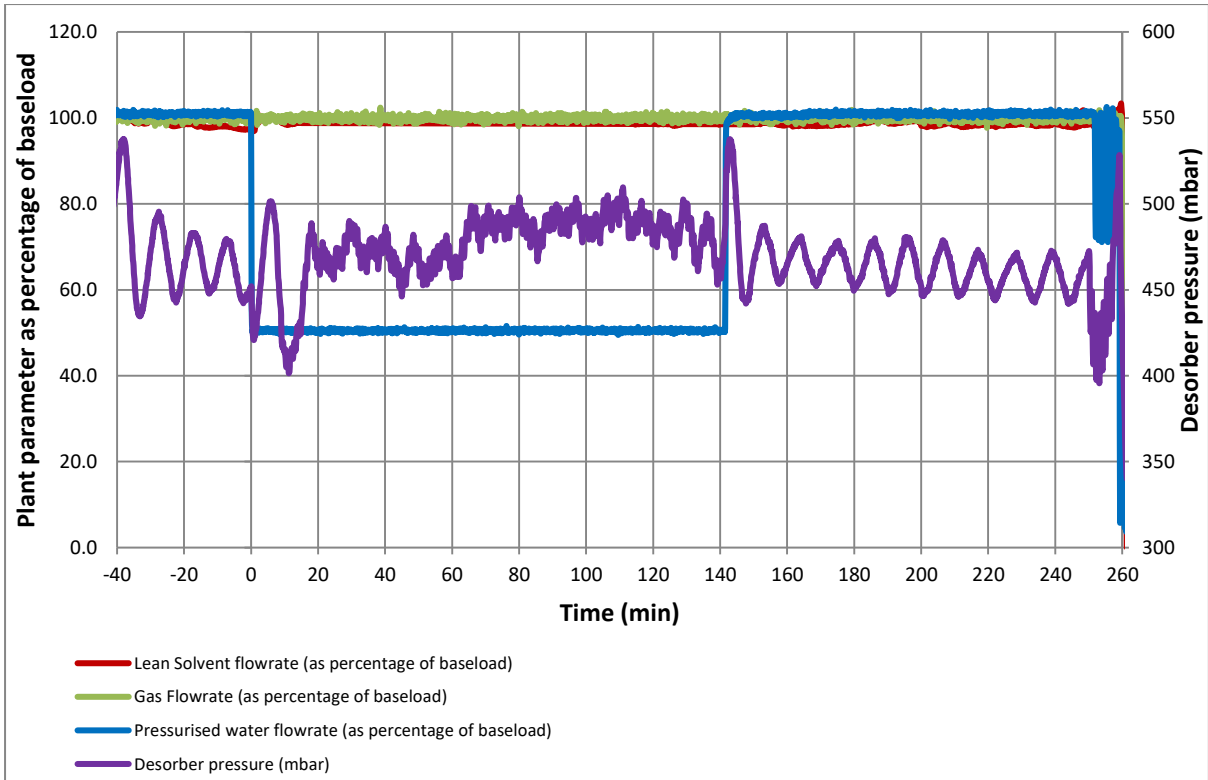
634

635

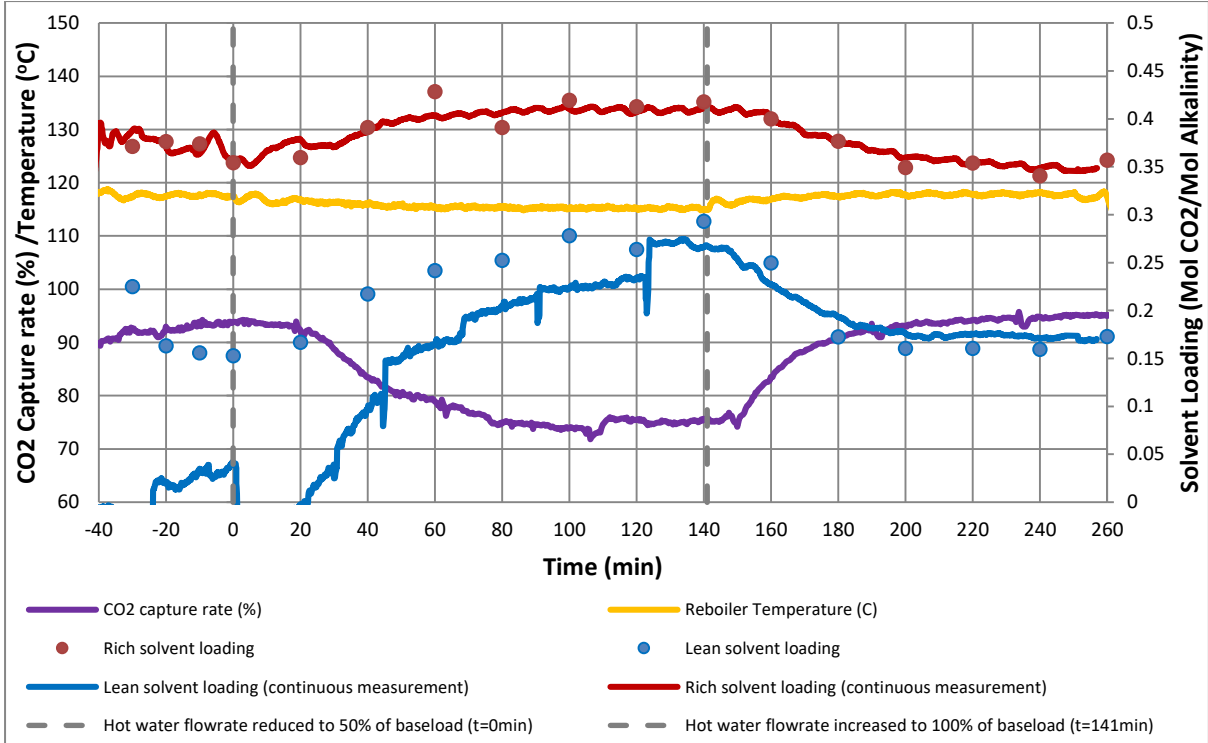
636

637

638

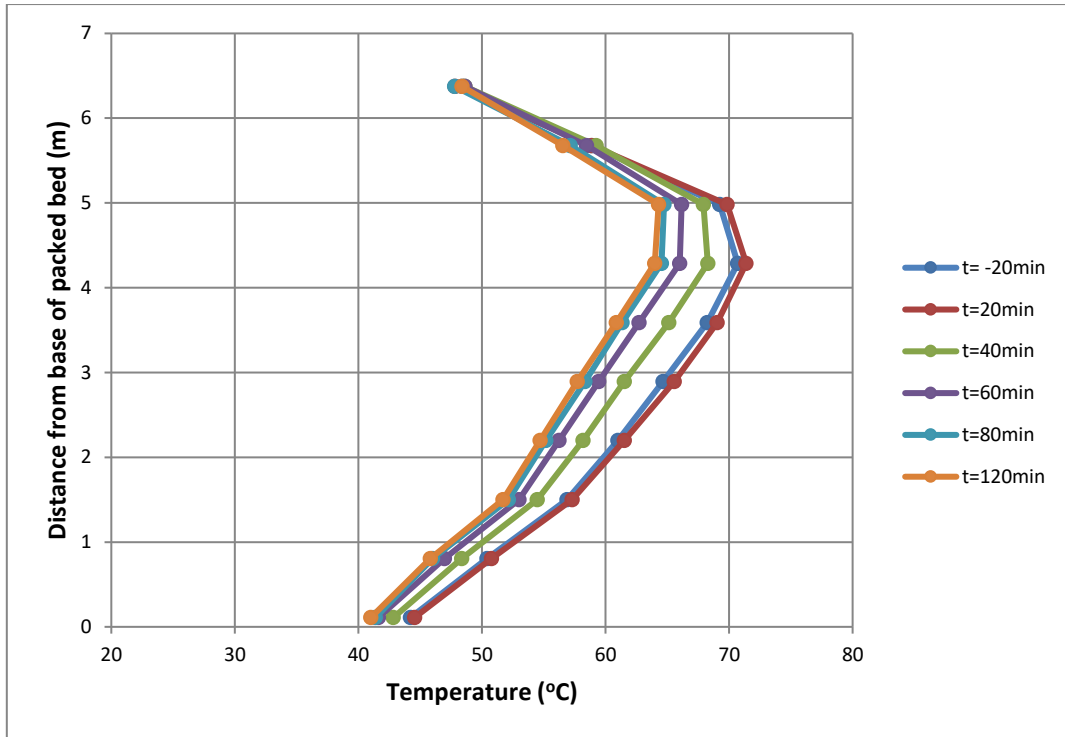


639



640  
641  
642  
643  
644  
645

**Fig. 17a. Gas, solvent hot water flow rate and desorber pressure as percentage of baseload operation, frequency response scenario**  
**Fig. 17b. Rich and lean solvent loading, reboiler temperature and CO<sub>2</sub> capture efficiency, frequency response scenario**



646

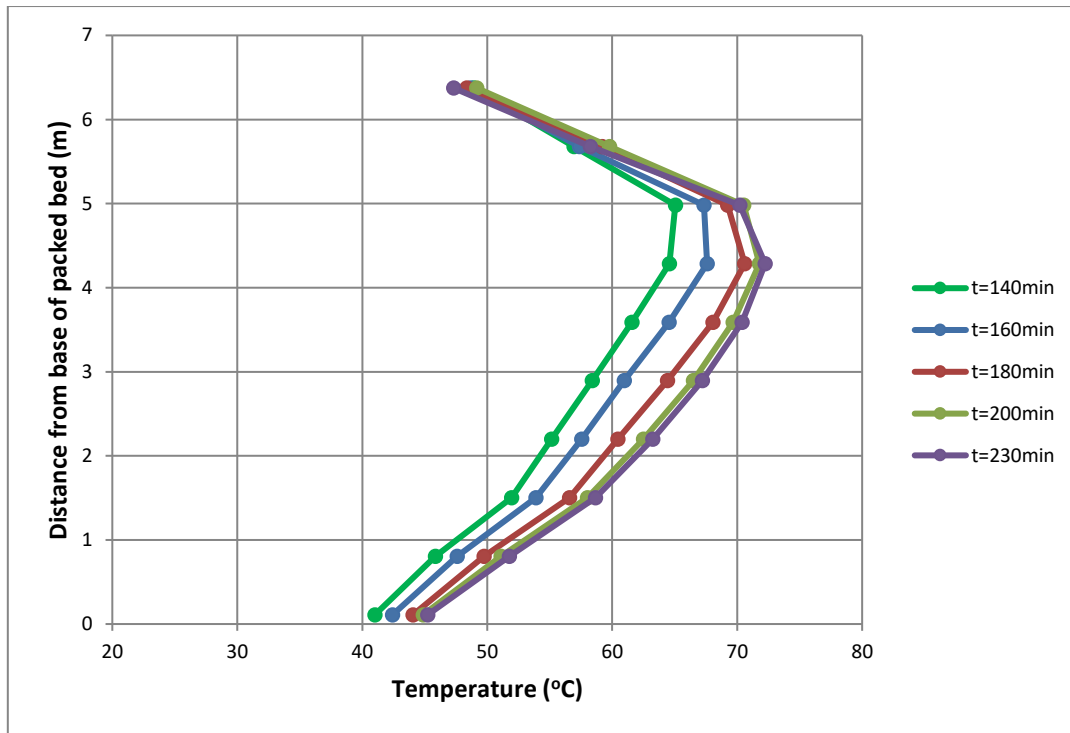


Fig. 18a. Absorber temperature profile, frequency response scenario,  $t = -10\text{min}$  to  $t = 100\text{min}$   
 Fig. 18b. Absorber temperature profile, frequency response scenario,  $t = -100\text{min}$  to  $t = 235\text{min}$

647  
 648  
 649  
 650

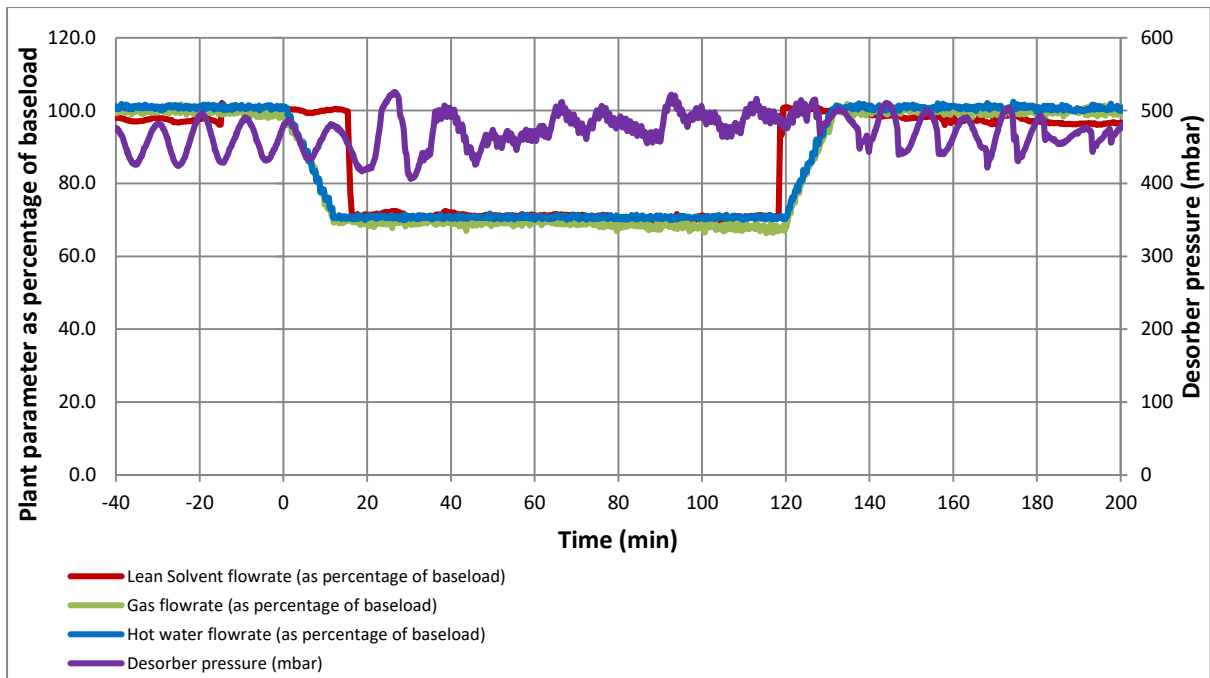
#### 4.6 Capture plant ramping

652 With increasing contribution to an electricity generation portfolio from intermittent renewable sources it  
 653 is likely that some coal-fired power stations will operate in a load-following regime for a significant  
 654 proportion of their operational lifetime. This scenario simulates the capture plant reducing its output from  
 655 baseload to 70%, then ramping back up to baseload after 2 hours. Gas flow is ramped down at 2.5% of  
 656 baseload ( $5\text{m}^3/\text{hr}$ ) per minute to represent a coal unit cycling rate of 2.5% of its output per minute (DECC,  
 657 2014). Hot water flow is also ramped down at 2.5% of baseload ( $0.25\text{m}^3/\text{hr}$ ) per minute (fig. 19a). Once

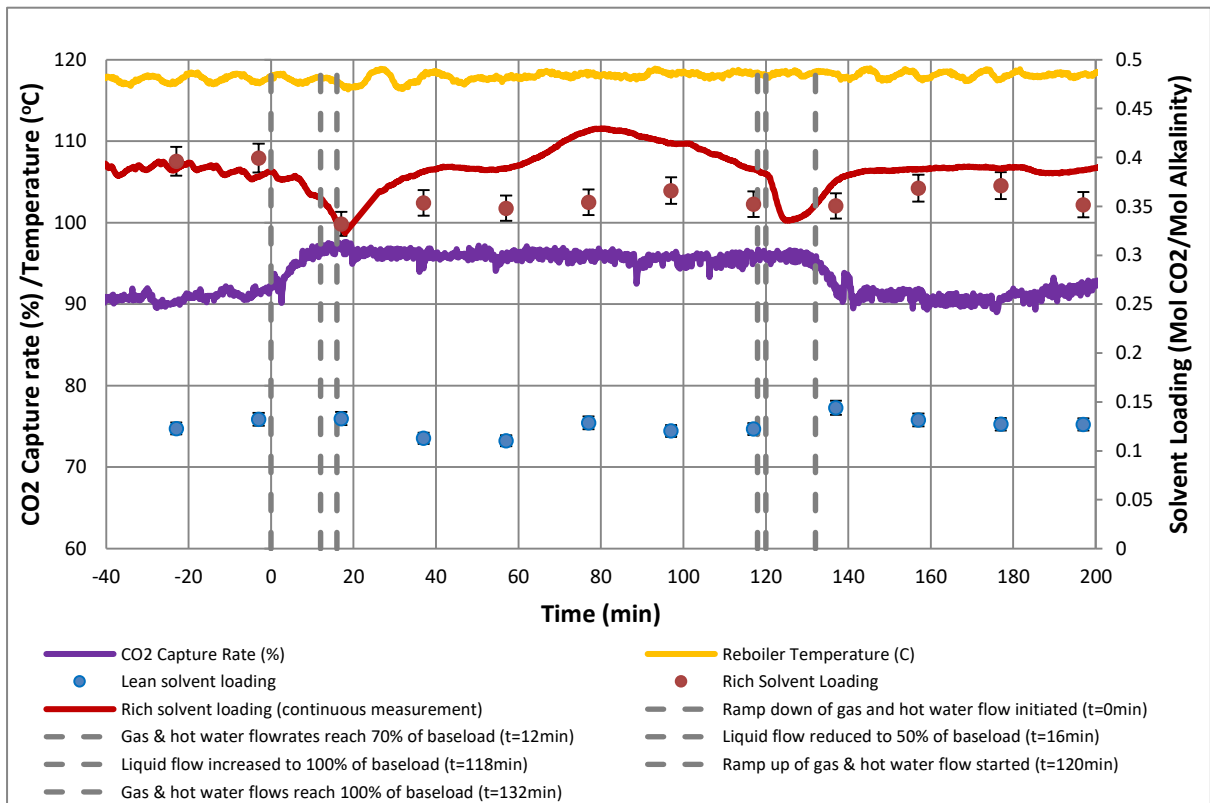
658 gas and hot water flows have been stabilised at 70% of baseload at t=12min a step-change in solvent flow  
659 from 100% to 70% of baseload (1000l/hr to 700l/hr) is made to keep the L/G ratio constant for as much  
660 of the operation as possible.

661 At t=119min the flow of solvent is increased to 100% of baseload operating conditions (1000l/hr) in  
662 anticipation of the gas and hot water ramp operation. At t=120min, gas and hot water flow are both ramped  
663 up at a rate of 2.5% of baseload per minute, then stabilised at baseload at t=132min (fig. 19a).

664 A slight increase in CO<sub>2</sub> capture efficiency from 90% to 96% is observed while the plant is operating at 70%  
665 capacity. This is the opposite of what is observed in the simulation of Mac Dowell and Shah (2015), who  
666 report a small decrease. The reason for this becomes clear if the gas and liquid flow rate during the load-  
667 following operation are inspected closely (fig. 19c). In the modelling study, the L/G flow ratio and both lean  
668 and rich loading are kept constant throughout. Due to the imperfect control system of the pilot plant, for a  
669 significant proportion of the real operation the L/G ratio is greater than at baseload, with liquid flow  
670 varying between 71-72% and gas flow at around 68-69%. The lean solvent loading also appears to decrease  
671 slightly over the duration of the event which may account for the higher capture efficiency during t=78-  
672 93min, when the L/G ratio is almost the same as at baseload flow conditions (fig. 19b). However, the change  
673 is small (around 0.01-0.02 mol/mol) and there is some variation in titration measurements both at  
674 baseload and during the ramping operation (titration points at t=-23min, t=77min). In the absence of  
675 accurate continuous lean loading measurements it is not possible to come to definitive conclusions about  
676 how this factor affects the capture efficiency.

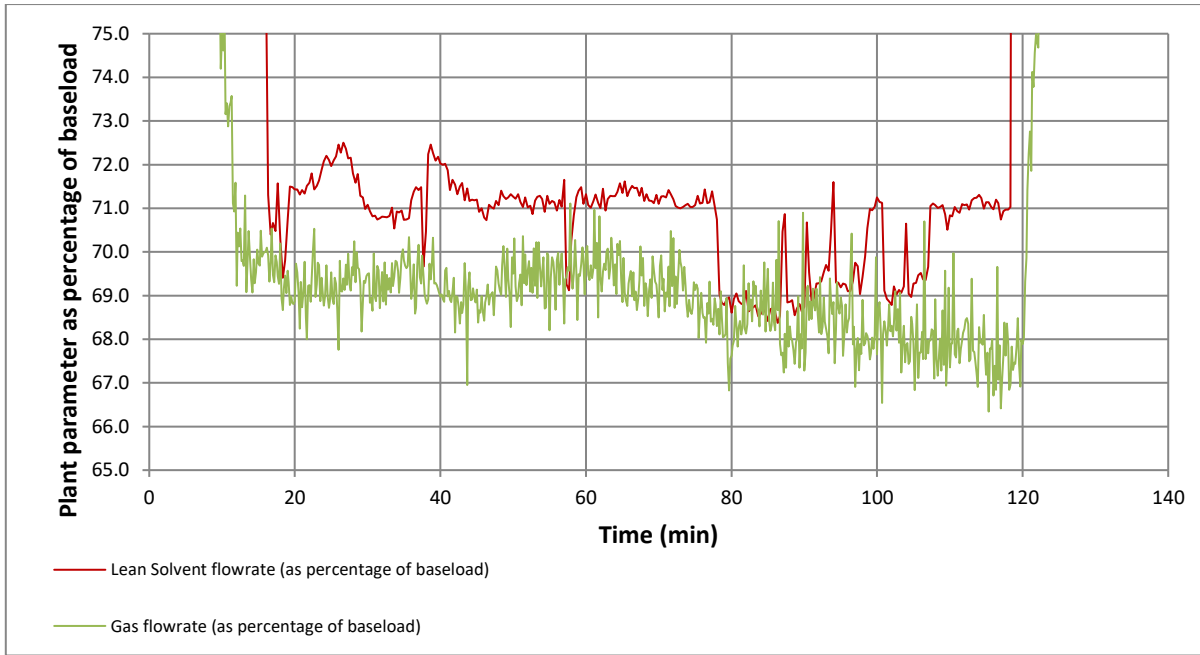


677



678





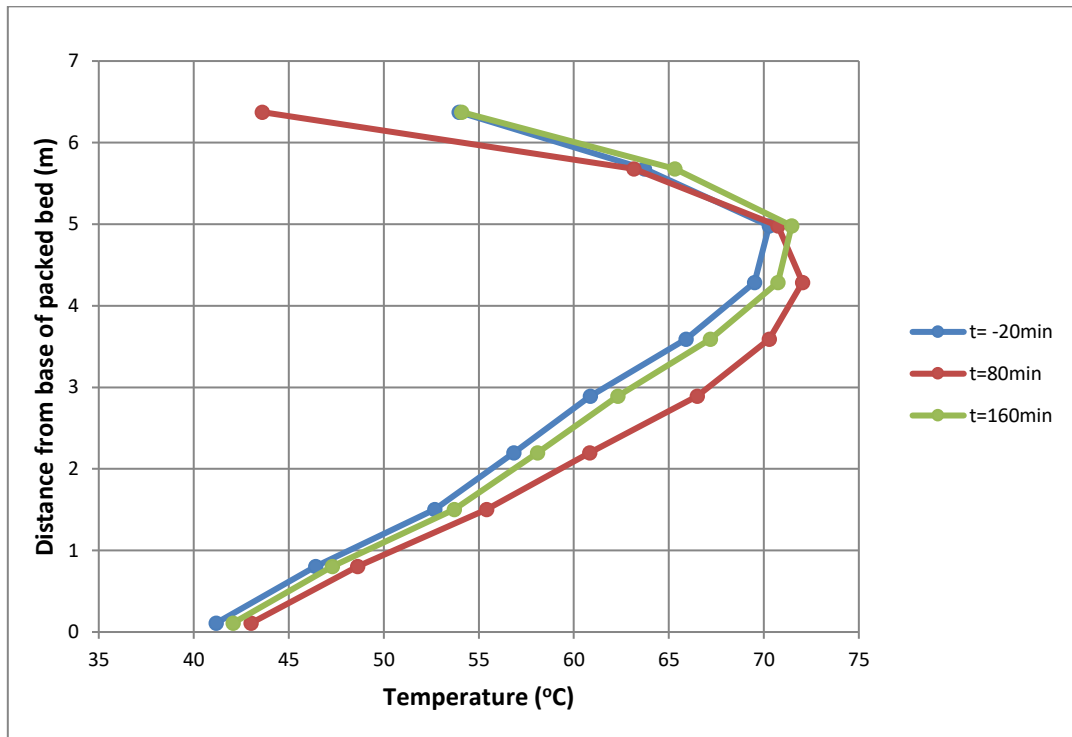
679  
 680  
 681  
 682  
 683  
 684  
 685  
 686  
 687  
 688  
 689  
 690

**Fig. 19a. Gas, solvent hot water flow rate and desorber pressure as percentage of baseload operation, load following scenario**

**Fig. 19b. Rich and lean solvent loading, reboiler temperature and CO<sub>2</sub> capture efficiency, load following scenario**

**Fig. 19c Gas and solvent flow rate as percentage of baseload operation, load following scenario**

The temperature bulge increases in magnitude slightly as a result of the increased capture efficiency and moves down the packed bed, indicating that a relatively higher proportion of CO<sub>2</sub> is being absorbed per unit of solvent at the absorber inlet (fig. 20). Once the plant is stabilised at baseload flow conditions after t=132min the capture efficiency decreases back to around 90%, as the L/G ratio returns to 5l/m<sup>3</sup>.



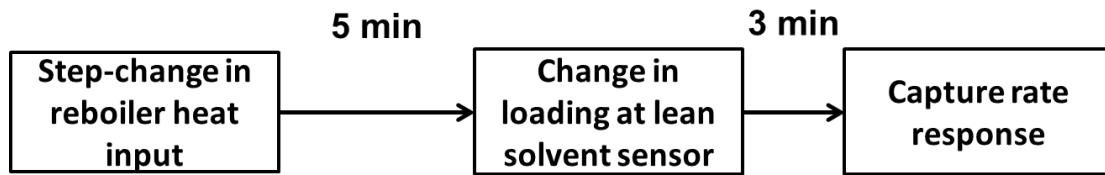
691  
 692  
 693

**Fig. 20 Absorber temperature profile, load following scenario**

694 There remains scope for the implementation of flexible load-following operations by using strategies such  
 695 flue gas venting, varying degrees of solvent regeneration and solvent storage. The idea is to maximise the  
 696 electricity available for export during peak selling times, while maintaining an average level of CO<sub>2</sub> capture  
 697 close to 90% over the course of a single day (Enaasen et al, 2016; Mac Dowell & Shah, 2015). These could  
 698 be investigated in future pilot-scale test campaigns on flexible CCS.  
 699

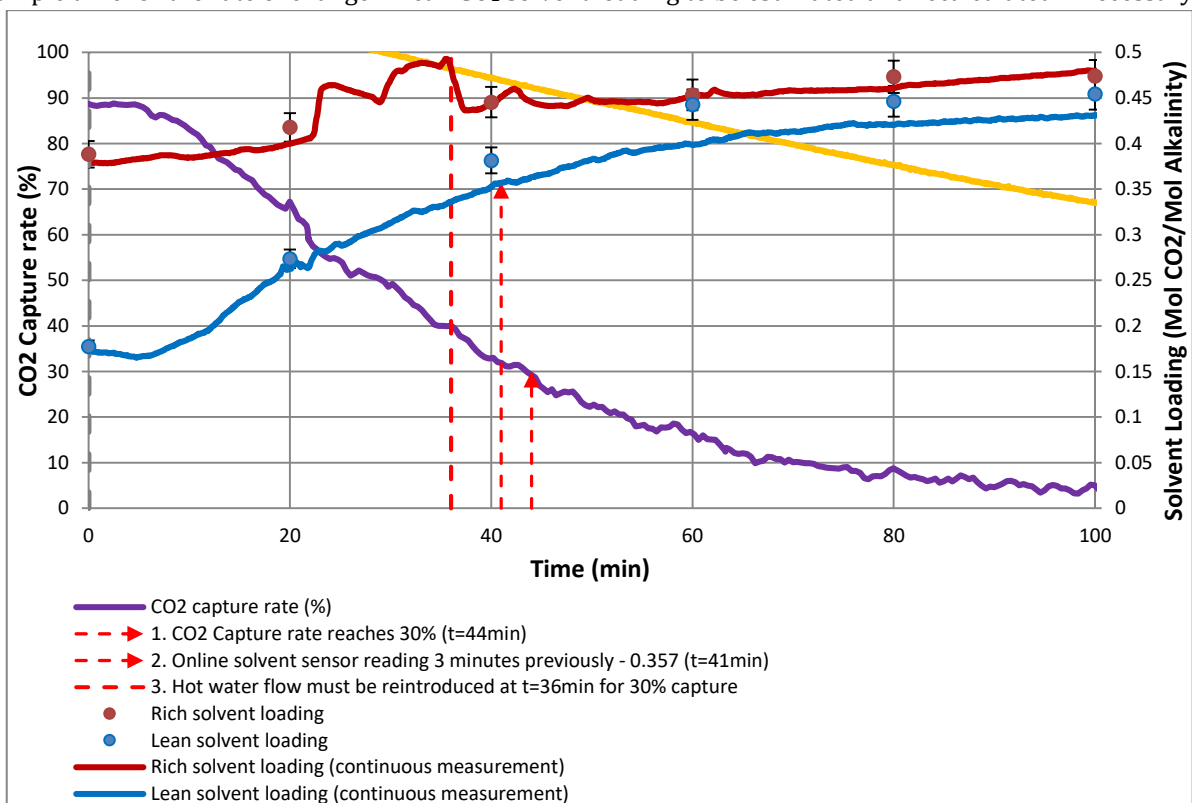
#### 700 4.7 Real-time control using online solvent measurement

701 In this scenario, control of the plant in real-time using online solvent measurements is demonstrated. It has  
 702 already been demonstrated (section 4.3) that at baseload solvent and gas flow rates, a response in lean  
 703 loading online measurement is observed approx. 5min after a step-change change in reboiler heat input.  
 704 The CO<sub>2</sub> capture efficiency responds after a further 3min (see table 5).



705 **Fig. 21 Capture efficiency and lean solvent response times at baseload solvent flow conditions**

706  
 707  
 708 This knowledge can be used to estimate the lean solvent loading which will result in a desired capture  
 709 efficiency by observing plant trends from previous scenarios. For the purpose of demonstration, a capture  
 710 efficiency of 30% was selected. In scenario 4.3 the capture efficiency reaches 30% at t=44min, this allows  
 711 ample time for the rate of change in lean CO<sub>2</sub> solvent loading to be estimated and recalculated if necessary.



712 **Fig. 22 Section of data between t=0 and t=100min from scenario 4.3**

713  
 714  
 715 With reference to a section of data from scenario 4.3 (fig. 22) and table 4, it is possible to retroactively  
 716 calculate when the flow of hot water to the reboiler should be reintroduced using the time at which the CO<sub>2</sub>  
 717 capture efficiency reaches 30%.

- 718 1. CO<sub>2</sub> capture efficiency reaches 30% at t=44min.

- 719 2. The solvent loading which corresponds to 30% capture passes through the lean solvent loading  
 720 analyser 3 minutes previously, at t=41min. At this time, lean loading is 0.357 mol MEA/mol CO<sub>2</sub>.  
 721 3. To achieve a maximum solvent loading of 0.357 mol MEA/mol CO<sub>2</sub> and hence a CO<sub>2</sub> capture  
 722 efficiency of 30% the flow of hot water to the reboiler must be reintroduced 5 minutes before (2.),  
 723 at t=36min.  
 724

725 The lean loading can be used to control the plant by calculating the rate of change of lean solvent based on  
 726 current trends and predicting its value in 5 minutes time. If this value exceeds the “target” lean loading of  
 727 0.357mol CO<sub>2</sub>/mol MEA the flow of hot water to the reboiler should be restarted. A simple Boolean  
 728 expression for the method in more general terms could look as follows:  
 729

$$730 \quad \text{If } \left( \alpha_{\text{current}} + \left( \Delta t_{\text{desorber-sensor}} * \frac{\Delta \alpha}{\Delta t} \right) > \alpha_{\text{target}} \right) \text{ Then} \quad \text{(Equation 3)}$$

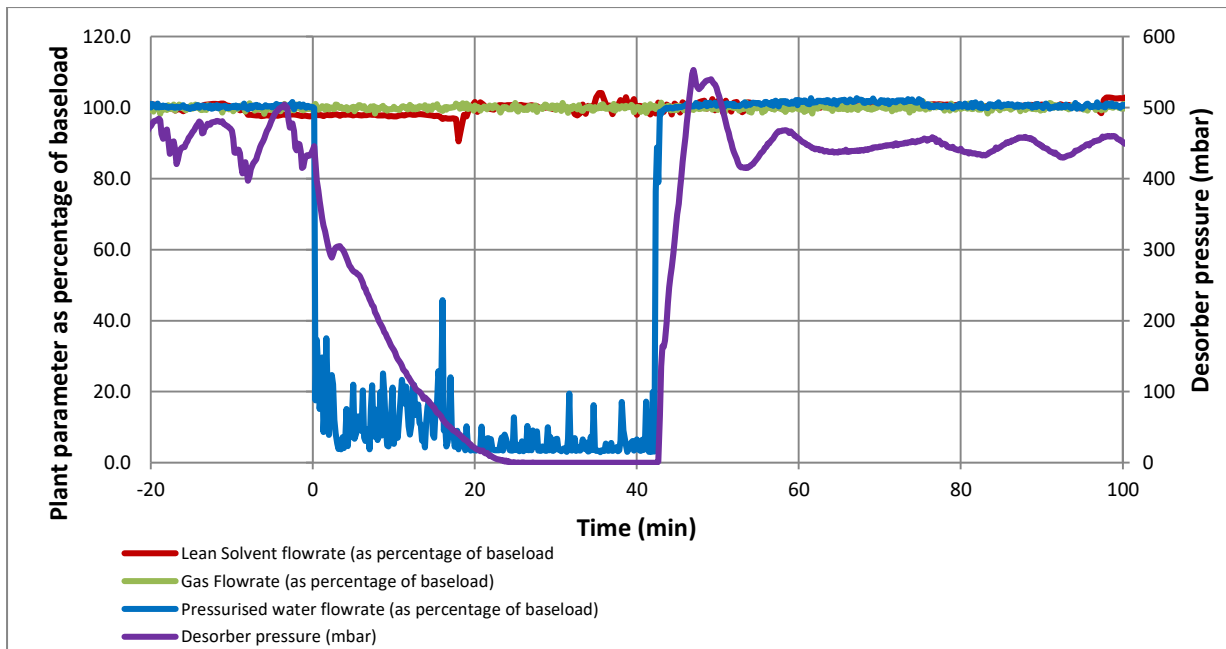
$$731 \quad \quad \quad (PV = 0)$$

$$732 \quad \text{Else}(PV = 1)$$

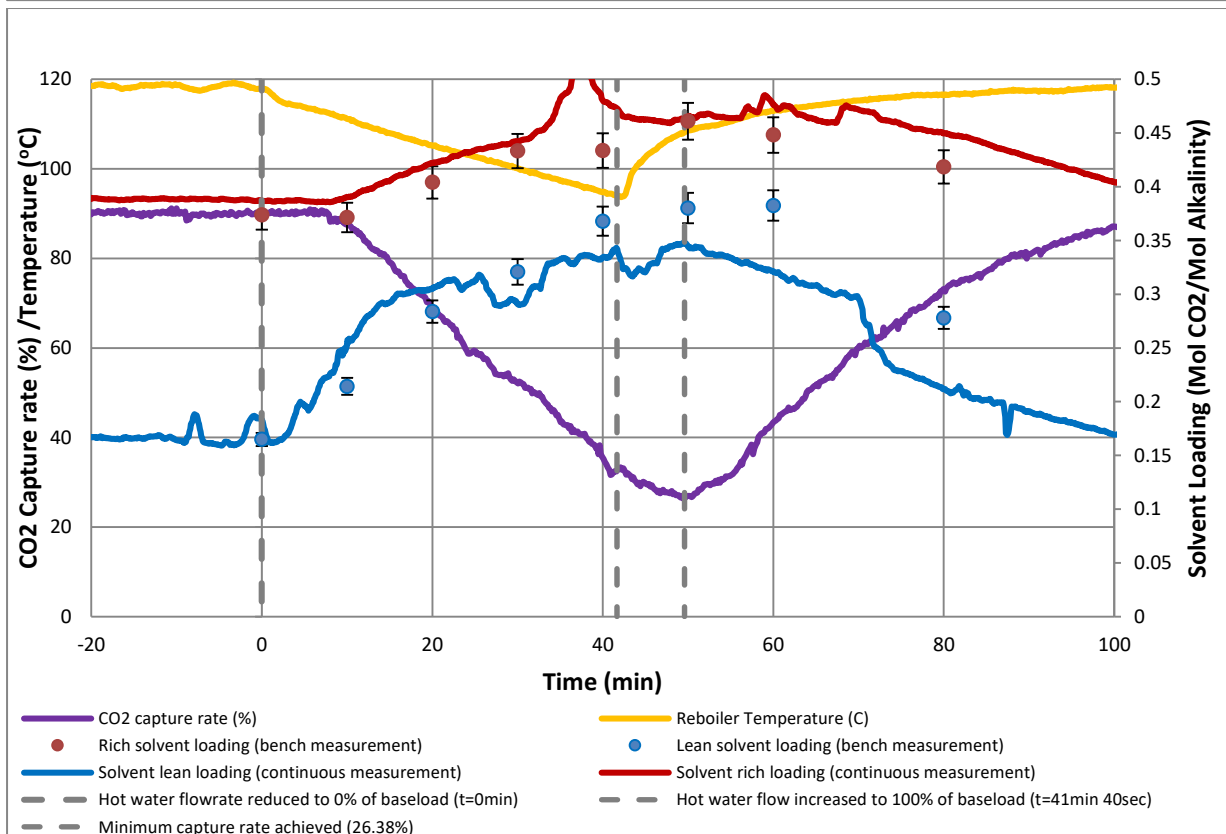
733  
 734 Where  $\alpha_{\text{current}}$  is the current online lean loading measurement,  $\Delta t_{\text{desorber-sensor}}$  is the time delay between  
 735 making a change in reboiler heat input and a response being observed in lean loading measurement,  $\frac{\Delta \alpha}{\Delta t}$  is  
 736 the lean loading’s rate of change (based on t=15min – t=25min in this case) and  $\alpha_{\text{target}}$  is the previously-  
 737 determined “target” lean loading. PV refers to the position of the hot water bypass valve, 0 being completely  
 738 open (all flow goes through the bypass), 1 being completely closed (all flow goes to the reboiler).

739 This is a fairly rudimentary method of lean loading and capture efficiency prediction. It could be improved  
 740 by taking into account dependencies on current plant temperatures (especially in the absorber), variations  
 741 in nominal amine concentration and planned changes in solvent flow rate. In future studies, rich online  
 742 solvent measurements could also be used as a predictor of how the rate of change in lean loading will vary  
 743 in the future. As the response of the lean loading upon reboiler shutdown is non-linear the rate of change  
 744 should be recalculated at regular intervals. This would require more plant data to be acquired than is  
 745 practical in the limited experimental time available, but future control efforts should consider these  
 746 dependencies and attempt to integrate the method with the plant control system.

747 Hot water flow to the reboiler is reduced to zero at t=0min (fig. 23a). The capture plant has no continuous  
 748 capture efficiency measurement as absorber gas inlet and outlet CO<sub>2</sub> concentrations are recorded on  
 749 separate FTIR machines, so plant control is dependent entirely on lean solvent measurements and the  
 750 prediction method. It is predicted that the loading will reach the target of 0.357 mol CO<sub>2</sub>/mol MEA at  
 751 t=46min, so the flow of hot water is redirected to the reboiler at t=41min. The plant operator and PID  
 752 controlled bypass valve require additional time to respond, and the flow of hot water to the reboiler  
 753 requires time to stabilise. In retrospect, this could have been compensated for. The hot water reaches its  
 754 baseload operating flowrate at approximately t=43min.  
 755



756



757  
758  
759  
760  
761  
762

**Fig. 23a. Gas, solvent hot water flow rate and desorber pressure as percentage of baseload operation, real time control with online solvent measurement**

**Fig. 23b. Rich and lean solvent loading, reboiler temperature and CO<sub>2</sub> capture efficiency, real time control via online solvent measurement**

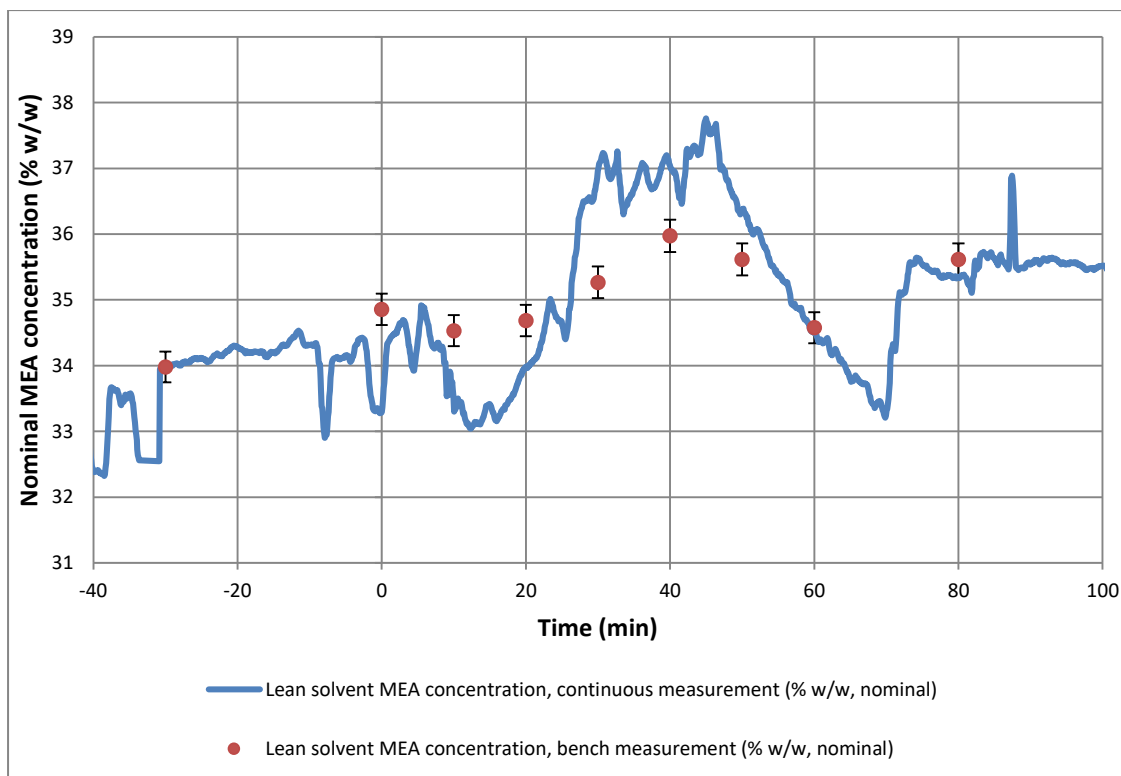
763 The target minimum capture efficiency is 30% and the actual capture efficiency achieved is 26.4%,  
764 displaying that while plant control using continuous online solvent measurements is possible there  
765 remains scope for improvement (Fig.23b). The rate of change of lean loading is estimated using the values  
766 at t=15 and t=25min. Titration measurements suggest that this resulted in an underestimation of  $\Delta\alpha/\Delta t$ ,  
767 leading to the optimum time for reintroduction of hot water being overshoot. A comparison between the

768 values of  $\Delta\alpha/\Delta t$  as predicted by continuous measurement and by bench titration is provided in table 6.  
 769 Although there is no titration point measurement at  $t=15\text{min}$  or  $t=25\text{min}$  an estimate can be made via linear  
 770 interpolation of the surrounding data points.

Lean loading data points used	Loading at $t=15\text{min}$	Loading at $t=25\text{min}$	$\Delta\alpha/\Delta t$	Predicted time to reach target lean loading	Predicted time to reintroduce hot water flow
Continuous measurement	0.292	0.313	0.0021	$t = 46\text{min}$	$t = 41\text{min}$
Interpolation of bench measurement	0.249	0.302	0.0053	$t = 35\text{min}$	$t = 30\text{min}$

771 **Table 6. Comparison of  $\Delta\alpha/\Delta t$  based on continuous measurements and interpolation of titration data**

772  
 773 Assuming that linear interpolation provides a sensible value of lean loading, the flow of hot water should  
 774 have been reintroduced approximately 11 minutes earlier during the experiment (figs 23a, b). The reasons  
 775 for the significantly higher solvent loading at  $t=15\text{min}$  shown in table 6 can be explained by comparing the  
 776 trends in nominal amine concentration for the online sensor and bench measurements (fig.24).  
 777



778 **Fig. 24 Continuous measurements of nominal amine concentration compared with titrations**

779  
 780 The data shows that the lean solvent sensor under-estimates nominal solvent amine concentration at  
 781  $t=15\text{min}$ . Lean loading at  $t=15\text{min}$  is overestimated in comparison with bench titration measurements,  
 782 accounting for the low value of  $\Delta\alpha/\Delta t$  calculated during the experiment (table 6). Due to the non-linearity  
 783 of the  $\text{CO}_2$  capture efficiency response a more robust method of achieving a target capture efficiency would  
 784 be to recalculate  $\Delta\alpha/\Delta t$  at regular intervals using Labview or similar control software, so it can be used as  
 785 a control variable in scenarios which are more complex and relevant to real plant operation than a simple  
 786 steam decoupling. The algorithm used by the online sensor to calculate lean loading could also be improved.  
 787 The measured values of lean loading using online measurement techniques (such as the one described in  
 788 the article) can be translated into rate of change of lean loading ( $\Delta\alpha/\Delta t$ ) which can be fed into a  
 789 PLC/labview code or any other process plant control software as a control variable. The live data of the  
 790 control variable coming from the plant then can be used to predictively control the plant.  
 791

792 Nevertheless, given the non-ideal operating environment and basic prediction method the sensor  
793 performed sufficiently well to achieve a minimum CO<sub>2</sub> capture efficiency within 4% of the target. To our  
794 knowledge, this is the first implementation of PCC plant control combined with in-situ online loading  
795 measurements reported in the public domain. It opens the door for the development of fit-for-purpose  
796 control strategy tools for dynamic operation, with further work focusing on the improvement of sensor  
797 performance and refinement of the prediction method.

798

## 799 **5. Conclusions and Key Findings**

800 Six flexible operating scenarios which could be encountered by operators of PCC as applied to coal-fired  
801 power plant are demonstrated. Via comparison of different methodologies for plant start-up, rapid  
802 introduction of steam to the reboiler is found to provide CO<sub>2</sub> emissions savings equivalent to 18.6% of the  
803 total daily emissions for a similar plant operating in a two-shifting dispatch pattern with 90% capture  
804 following startup (Table 3). Differences in plant construction are found to have a direct effect on solvent  
805 circulation times and as a result, how the plant reacts to dynamic operations. In contrast to the  
806 absorption/desorption facility described in Tait et al. (2016) which has a desorber outlet to absorber inlet  
807 solvent circulation time of 15-25mins, the PACT pilot facility used in this work has a circulation time of  
808 approx. 8mins. Changes in capture efficiency are observed after a relatively short period of time after  
809 making changes to reboiler heat input at the PACT pilot, but the increase or decrease is gradual and no  
810 significant additional fluctuations are observed following the initial return to baseload flow conditions, as  
811 the solvent becomes more rapidly mixed in the large desorber tank and sump. Steady state data and full  
812 datasets from these six dynamic tests are available via open access as supplementary material to this paper,  
813 for the potential validation of dynamic models. Tables of information which detail plant dimensions and  
814 packing types are also provided.

815 A final dynamic operating scenario demonstrates plant control uses real-time measurement of solvent  
816 loading to attempt to hit a “target” CO<sub>2</sub> capture efficiency following a steam shutdown event. A capture  
817 efficiency of 26.4% is achieved for a target of 30%. While not possible during this campaign due to time  
818 constraints, the next immediate steps for development of CO<sub>2</sub> capture efficiency control using online  
819 solvent measurements are as follows:

820

- 821 • Write Labview code (or other control software) which allows the existing prediction method  
822 to be implemented programmatically, with rate of change in solvent loading ( $\Delta\alpha/\Delta t$ ) being  
823 recalculated on a regular basis.
- 824 • Refine the sensor algorithm which calculates solvent loading to make measurements more  
825 reliable, accurate and less prone to instability. Additional studies at pilot-facilities and large-  
826 scale commercial CCS plants which are not published at the time of writing show considerable  
827 improvements in sensor stability, and consistent close agreement with offline measurements.  
828 These results are to be presented at the GHGT-14 conference.
- 829 • Continue to develop knowledge of plant hydrodynamics so that the prediction method can be  
830 scaled to account for changes in solvent flow rate.

831

832 Achievement of these objectives at the UKCCSRC PACT amine pilot can form a basis for the development of  
833 an enhanced plant control system, which uses continuous solvent measurements as control variables to  
834 maintain plant parameters within pre-defined boundaries. Differences in plant construction are found to  
835 significantly affect response to dynamic operation, so a step-by-step methodology for the development of  
836 similar control systems at other plants is likely to be a useful tool.

837 Solvent working capacity as a potential control variable was discussed by Tait et al. (2016) but it is now  
838 obvious that this is too simplistic an approach. Discrete knowledge of plant hydrodynamics, response times  
839 based on current plant conditions, knowledge of upcoming changes in generation plant output and  
840 continuous monitoring of rich and lean solvent loading will be required to optimise operation. Advanced  
841 process control system architectures such as Model-predictive control (MPC) and fuzzy logic control  
842 applied to the control of post-combustion capture are a promising alternative to single input-single output

843 PID or cascading-PID control systems in maintaining plant operation within environmental, economic and  
844 operational boundaries via active control of solvent flow, desorber pressure and reboiler energy input (Luu  
845 et al., 2015; Mechleri, 2015). The successful demonstration of the sensor represents a significant practical  
846 step toward combining online solvent measurements with novel control strategies to optimise plant  
847 operation.

848

849 To summarise, the key findings of this work are:

850 • Six dynamic pilot-scale datasets are generated and provided as supplementary material to this  
851 work for the potential validation of dynamic plant models.

852 • Two plant startup modes are implemented at pilot-scale.

853 ○ Startup method 1: The low pressure steam turbine is powered up before stripping steam  
854 is sent to the reboiler.

855 ○ Startup method 2: Low pressure steam is immediately introduced to the reboiler as soon  
856 as it becomes available.

857 Total CO<sub>2</sub> emissions during startup are 25.1kg for method 1 and 10.3kg for method 2, a saving of  
858 14.8kg. To quantify these potential savings, the case of a two-shifting coal plant which initiates a  
859 hot startup at 6am, operates with 90% capture efficiency for the rest of the day and shuts down at  
860 10pm is considered. Total residual CO<sub>2</sub> emissions for a plant of this scale over the 16hr period are  
861 79.4kg with startup method 1, and 64.6kg with startup method 2. This represents a potential  
862 18.6% reduction in daily emissions, at the cost of increased low-pressure steam consumption  
863 during startup.

864 • A steam shutdown event is used to determine response times critical plant response times, with  
865 the intent of using continuous online solvent measurements as an input parameter for the control  
866 of CO<sub>2</sub> capture efficiency.

867 • In the final dynamic scenario, we demonstrate the use of an online solvent sensor combined with  
868 knowledge of plant response times to achieve an arbitrarily chosen “target” capture efficiency  
869 following a steam shutdown event. For a target of 30%, a minimum capture efficiency of 26.4% is  
870 achieved.

871

872

873

## 874 **Acknowledgement**

875 Financial and technical support for the operation of the pilot-scale facility from UK Carbon Capture  
876 Research PACT facility is gratefully acknowledged, as is financial support from a UK Carbon Capture  
877 Research Centre funded project (UKCCSRC-C2-214). The online sensors used in this work were developed  
878 with funding from Doosan Power Systems and the Energy Technology Partnership (ETP).

879

880

## 881 **Glossary of Terms**

882 Cp – Specific heat capacity (J/kg.K)

883 m – Mass flow rate (kg/s)

884 Q<sub>reb</sub> – Reboiler heat duty (GJ/tCO<sub>2</sub>)

885 T – Temperature (°C)

886 t – Time (min)

887 α – Solvent CO<sub>2</sub> loading (mol CO<sub>2</sub>/mol alkalinity)

888 η – CO<sub>2</sub> capture efficiency (% , mass basis)

889 ρ – Density (kg/m<sup>3</sup>)

890 φ – Volume fraction

891

## 892 **References**

893 Akram, M. (2017). Amine Plant Layout. Personal communication, 28/03/17.

894 Akram, M., Ali, U., Best, T., Blakey, S., Finney, K.N. and Pourkashanian, M. (2016). Performance evaluation of  
895 PACT Pilot-plant for CO<sub>2</sub> capture from gas turbines with Exhaust Gas Recycle. *International Journal of*  
896 *Greenhouse Gas Control*, 47, 137-150.

897 Bui, M., Gunawan, I., Verheyen, V., Feron, P., Meuleman, E. and Adeloju, S. (2015). Dynamic modelling and  
898 optimisation of flexible operation in post-combustion CO<sub>2</sub> capture plants – a review. *Computers and*  
899 *Chemical Engineering*, 61, 245-265.

900 Buschle, W. (2015). Solvent analysis instrumentation options for the control and flexible operation of post  
901 combustion carbon dioxide capture plants. PhD thesis, The University of Edinburgh.

902 Ceccarelli, N., van Leeuwen, M., van Leeuwen, P., Maas, W., Ramos, A., van der Vaart, R. and Wolf, T. (2014).  
903 Flexibility of low-CO<sub>2</sub> gas power plants: Integration of the CO<sub>2</sub> capture unit with CCGT operation. *Energy*  
904 *Procedia*, 63, 1703-1726.

905 Chalmers, H., Leach, M., Lucquiaud, M. and Gibbins, J. (2009). Valuing flexible operation of power plants  
906 with CO<sub>2</sub> capture. *Energy Procedia*, 1, 4289-4296.

907 Davison, J. (2006). Performance and costs of power plants with capture and storage of CO<sub>2</sub>. *Energy*, 32,  
908 1163-1176.

909 Department for Energy and Climate Change and Parsons Brinckerhoff. 2014. Technical Assessment of the  
910 Operation of Coal & Gas Fired Plants. Retrieved from  
911 [https://www.gov.uk/government/uploads/system/uploads/attachment\\_data/file/387566/Technical As](https://www.gov.uk/government/uploads/system/uploads/attachment_data/file/387566/Technical_Assessment_of_the_Operation_of_Coal_and_Gas_Plant_PB_Power_FIN....pdf)  
912 [sessment of the Operation of Coal and Gas Plant PB Power FIN....pdf](https://www.gov.uk/government/uploads/system/uploads/attachment_data/file/387566/Technical_Assessment_of_the_Operation_of_Coal_and_Gas_Plant_PB_Power_FIN....pdf)

913 Errey, O., Chalmers, H., Lucquiaud, M. and Gibbins, J. (2014). Valuing responsive operation of post-  
914 combustion CCS power plants in low carbon electricity markets. *Energy Procedia*, 63, 7471-7484.

915 Flø, N.E., Kvamsdal, H.M. and Hillestad, M. (2016). Dynamic simulation of post-combustion CO<sub>2</sub> capture for  
916 flexible operation of the Brindisi pilot plant. *International Journal of Greenhouse Gas Control*, 48, 204-215.

917 Haines, M.R. and Davison, J. (2014). Enhancing dynamic response of power plant with post-combustion  
918 capture using “Stripper stop”. *International Journal of Greenhouse Gas Control*, 20, 49-56.

919 IPCC (2014). *Climate Change 2014: Fifth Assessment Report of the Intergovernmental Panel on Climate*  
920 *Change*. Cambridge University Press: Cambridge, UK

921 International Energy Agency (2015). World Energy Outlook 2015. OECD/IEA: Paris, France.

922 Lawal, A., Wang, M., Stephenson, P. Koumpouras, G. and Yeung, H. (2010). Dynamic modelling and analysis  
923 of post-combustion CO<sub>2</sub> chemical absorption process for coal-fired power plants. *Fuel*, 89, 2791-2801.

924 Lucquiaud, M., Chalmers, H. and Gibbins, J. (2009). Capture-ready supercritical coal-fired power plants and  
925 flexible post-combustion CO<sub>2</sub> capture. *Energy Procedia*, 1, 1411-1418.

926 Luu, M.T., Manaf, N.A. and Abbas, A. (2015). Dynamic modelling and control strategies for flexible operation  
927 of amine-based post-combustion CO<sub>2</sub> capture systems. *International Journal of Greenhouse Gas Control*, 39,  
928 377-389.

929 Mac Dowell, N. and Staffell, I. (2016). The role of flexible CCS in the UK’s future energy system. *International*  
930 *Journal of Greenhouse Gas Control*, 48, 327-344.

931 Mac Dowell, N. and Shah, N. (2014). Optimisation of post-combustion CO<sub>2</sub> capture for flexible operation.  
932 *Energy Procedia*, 63, 1525-1535.

933 Mangiaracina A., Zangrilib L., Robinsonc L.\*, Kvamsdald H.M., Van Ose P. (2014). OCTAVIUS: Evaluation  
934 of flexibility and operability of amine based post combustion CO<sub>2</sub> capture at the Brindisi Pilot Plant, *Energy*  
935 *Procedia* 63 ( 2014 ) 1617 – 1636.

936 Mechleri, E. (2015). Controllability analysis of a post-combustion CO<sub>2</sub> capture plant integrated with a coal  
937 and natural gas-fired power plan. 3rd Post Combustion Capture Conference, 9th September 2015, Regina,  
938 Canada.

939 National Energy Technology Laboratory (2013, September 2013), *Cost and Performance Baseline for Fossil*  
940 *Energy Plants Volume 1: Bituminous Coal and Natural Gas to Electricity*, retrieved from:  
941 [http://www.netl.doe.gov/File%20Library/Research/Energy%20Analysis/OE/BitBase FinRep\\_Rev2a-](http://www.netl.doe.gov/File%20Library/Research/Energy%20Analysis/OE/BitBase_FinRep_Rev2a-3_20130919_1.pdf)  
942 [3\\_20130919\\_1.pdf](http://www.netl.doe.gov/File%20Library/Research/Energy%20Analysis/OE/BitBase_FinRep_Rev2a-3_20130919_1.pdf)

943 Partnership to Advance Clean Energy (2014, February 2014), *Best Practices Manual for Indian*  
944 *Supercritical Plants*, retrieved from: [http://www.pace-d.com/wp-content/uploads/2013/03/BP-](http://www.pace-d.com/wp-content/uploads/2013/03/BP-MANUAL-FOR-PRINTING.pdf)  
945 [MANUAL-FOR-PRINTING.pdf](http://www.pace-d.com/wp-content/uploads/2013/03/BP-MANUAL-FOR-PRINTING.pdf)



946 Tait, P, Buschle, W, Ausner, I, Wehrli, M, Valluri, P and Lucquiaud, M. (2016). A pilot-scale study of  
947 dynamic response scenarios for the flexible operation of post-combustion CO<sub>2</sub> capture. *International*  
948 *Journal of Greenhouse Gas Control*, 216-233.

949 van Eckeveld, A. C., van der Ham, L. V., Geers, L. F. G., van den Broeke, L. J. P., Boersma, B. J. & Goetheer, E. L.  
950 V. (2014). Online monitoring of the solvent and absorbed acid gas concentration in a CO<sub>2</sub> capture process  
951 using monoethanolamine. *Industrial & Engineering Chemistry Research*, 53, 5515-5523.

952 Wonder, D.K., Blake, R.J., Fager, J.H. and Tierney, J.V. (1959). An Approach to Monoethanolamine Solution  
953 Control: Chemical Analysis and its Interpretation. In Laurance Reid Gas Conditioning Conference.  
954 Norman, Oklahoma, USA, pp. 42-59.